Research Paper

LEDGIN-mediated Inhibition of Integrase–LEDGF/p75 Interaction Reduces Reactivation of Residual Latent HIV

Lenard S. Vranckx [a], Jonas Demeulemeester [a], Suha Saleh [a], Annegret Boll [b], Gerlinde Vansant [a], Rik Schrijvers [a,c], Caroline Weydert [a], Emilie Battivelli [d], Eric Verdin [d], Anna Cereseto [b], Frauke Christ [a], Rik Gijsbers [a,1], Zeger Debyser [a,*,1]

[a] Laboratory of Molecular Virology and Gene Therapy, Department of Pharmacological and Pharmaceutical Sciences, KU Leuven, Kapucijnenvoer 33 VTCB +5, 3000 Leuven, Flanders, Belgium
[b] Laboratory of Molecular Virology, Centre for Integrative Biology (CIBIO), University of Trento, Via delle Regole 101, 38123 Trento, Italy
[c] Laboratory of Clinical Immunology, Department of Microbiology and Immunology, KU Leuven, Herestraat 49, 3000 Leuven, Flanders, Belgium
[d] Gladstone Institute of Virology and Immunology, University of California, 1650 Owens St., 94158 San Francisco, CA, USA

ARTICLE INFO

ABSTRACT

Persistence of latent, replication-competent Human Immunodeficiency Virus type 1 (HIV-1) provirus is the main impediment towards a cure for HIV/AIDS (Acquired Immune Deficiency Syndrome). Therefore, different therapeutic strategies to eliminate the viral reservoirs are currently being explored. We here propose a novel strategy to reduce the replicating HIV reservoir during primary HIV infection by means of drug-induced retargeting of HIV integration. A novel class of integration inhibitors, referred to as LEDGINs, inhibit the interaction between HIV integrase and the LEDGF/p75 host cofactor, the main determinant of lentiviral integration site selection. We show for the first time that LEDGF/p75 depletion hampers HIV-1 reactivation in cell culture. Next we demonstrate that LEDGINs relocate and retarget HIV integration resulting in a HIV reservoir that is refractory to reactivation by different latency-reversing agents. Taken together, these results support the potential of integrase inhibitors that modulate integration site targeting to reduce the likeliness of viral rebound.

1. Introduction

Combination antiretroviral therapy (cART) has revolutionized the treatment of HIV/AIDS, turning a life-threatening disease into a chronic illness. Yet, current therapies fail to cure infection due to the existence of a reservoir of latently infected cells (Archin et al., 2014; Bruner et al., 2015; Siliciano and Siliciano, 2015). While the Human Immunodeficiency Virus type 1 (HIV-1) actively replicates in activated CD4+ T lymphocytes, it is able to reside in a long-lived quiescent state, mainly in resting memory CD4+ T cells (Chun et al., 1997a,b; Finzi et al., 1997). This latently infected cell population is established early on during infection and consists of a small fraction of the resting CD4+ T cells in patients (about 1 in 10^6 cells) (Chun et al., 1997a,b; Finzi et al., 1997). The reservoir enables HIV persistence during cART and is responsible for the rebound of viremia upon therapy cessation (Richman et al., 2009). However, recent evidence suggests that persistent HIV-1 replication occurs in lymphoid tissue reservoirs due to insufficient drug penetration (Lorenzo-Redondo et al., 2016). Lentiviruses, such as HIV-1, preferentially integrate into transcriptionally active units (Schroder et al., 2002). The latter integration preference is retained in latently HIV-1 infected primary CD4+ T cells from patients (Han et al., 2004; Liu et al., 2006; Shan et al., 2011) and determined by Lens Epithelium-Derived Growth Factor (LEDGF/p75), a host-cell cofactor binding HIV-1 IN via its C-terminal protein binding domain (Integrase Binding Domain (IBD)) (Cherepanov et al., 2003, 2005) and reading chromatin through its PWWP domain (Eidahl et al., 2013; Pradeepa et al., 2012). LEDGF/p75 depletion shifts lentiviral integration out of transcription units (Ciuffi et al., 2005), a phenotype even more pronounced in human LEDGF/p75 knockout (KO) cells (Fadel et al., 2014; Schrijvers et al., 2012a; Shun et al., 2007). In the absence of LEDGF/p75, its paralogue HRP-2 can at least in part take over this targeting role for HIV integration (Schrijvers et al., 2012a,b; Wang et al., 2012).

Structure-based drug design targeting the well-defined interface (Cherepanov et al., 2005) between the IBD and the HIV-1 IN catalytic core resulted in the development of 2-(quinolin-3-yl)acetic acid

* Corresponding author at: Molecular Virology and Gene Therapy, KU Leuven, Kapucijnenvoer 33, VCTB +5, 3000, Flanders, Belgium.
E-mail addresses: Lenard.vranckx@med.kuleuven.be (L.S. Vranckx), Jonas.Demeulemeester@med.kuleuven.be (J. Demeulemeester), suha.saleh@kuleuven.be (S. Saleh), annegret.boll@gmail.com (A. Boll), Gerlinde.vansant@kuleuven.be (G. Vansant), Rik.schrijvers@kuleuven.be (R. Schrijvers), Caroline.weydert@med.kuleuven.be (C. Weydert), emilie.battivelli@gladstone.ucsf.edu (E. Battivelli), eric.verdin@gladstone.ucsf.edu (E. Verdin), anna.cereseto@unitn.it (A. Cereseto), Frauke.Christ@med.kuleuven.be (F. Christ), Rik.Gijsbers@med.kuleuven.be (R. Gijsbers), Zeger.debyser@med.kuleuven.be (Z. Debyser).
[1] Shared last authorship.

derivatives that inhibit HIV-1 replication (Christ et al., 2010). This novel class of antivirals is referred to as LEDGINs (Christ and Debyser, 2013; Christ et al., 2010, 2012; Debyser et al., 2015; Demeulemeester et al., 2014a). Novel congeners with nanomolar activity act as allosteric inhibitors, preventing the binding of both LEDGF/p75 and HRP-2 and interfering with the catalytic activity of IN (i.e. the so-called 'early effect') (Christ et al., 2012; Kessl et al., 2012; Tsiang et al., 2012). Recently, LEDGINs were found to inhibit late stage HIV replication as well (i.e. the 'late effect') (Balakrishnan et al., 2013; Desimmie et al., 2013; Jurado et al., 2013; Le Rouzic et al., 2013). The phenotype requires the binding of LEDGINs to the LEDGF/p75 binding pocket in IN (Desimmie et al., 2013; Le Rouzic et al., 2013) and is mediated by enhanced multimerisation of IN in the viral particles (Balakrishnan et al., 2013; Borrenberghs et al., 2014; Desimmie et al., 2013; Jurado et al., 2013). Contradictory results have been obtained as to whether LEDGINs affect the integration site distribution (Feng et al., 2016; Gupta et al., 2014; Sharma et al., 2014). In any case LEDGIN treatment results in a steep dose-dependent inhibition of viral replication in cell culture, supporting their clinical development (Fader et al., 2014; Fenwick et al., 2014).

Here we investigated the early effect of LEDGINs and evaluated their effect on HIV integration site distribution. In addition, we monitored the effect of LEDGINs on the establishment of the latent reservoir and investigated whether retargeting of integration could lead to a silent HIV reservoir resistant to reactivation. In a stepwise approach we first demonstrate that LEDGF/p75 depletion results in reduced integration and a quiescent state of residual integrants. Next, we demonstrate that upon treatment with LEDGINs, blocking the LEDGF/p75–IN interaction, the residual proviral integration shifts away from transcription units. LEDGIN treatment also shifts the 3D localization of the integrated provirus towards the inner nucleus. LEDGIN-induced retargeting results in a silent HIV reservoir in cell lines and primary CD4+ cells. This silent reservoir is refractory to reactivation by latency reversing agents (LRAs). Pushing sufficient proviruses into latency is theoretically predicted to drive the basic reproduction number of HIV below 1, resulting in unsustainable infection (Rouzine et al., 2015). Hence, addition of LEDGINs to cART regimens during acute HIV infection may represent a new strategy to achieve a remission of HIV infection in patients.

2. Materials and Methods

2.1. Cell culture, Virus Production and Transduction

All cells were tested to be mycoplasma free. Cells were cultured in a humidified atmosphere containing 5% CO_2 at 37 °C. SupT1 (provided by the National Institutes of Health (NIH) Reagent Program, NIH, Bethesda, MD). Nalm cells obtained from ATCC (Schrijvers et al., 2012a) were cultured in RPMI medium (GIBCO-BRL) supplemented with 10% v/v heat inactivated fetal calf serum (FCS, Sigma-Aldrich) and 0.01% v/v gentamicin (GIBCO). HEK293T cells (gift from O. Danos, Evry, France) were cultured in Dulbecco Modified Eagle Medium (DMEM, GIBCO) with 5% v/v FCS (Sigma-Aldrich) and 0.01% v/v gentamicin (GIBCO). U2OS cells (ATTC) were cultured in DMEM (GIBCO) with 10% v/v FCS. Vesicular stomatitis virus G (VSV-G)-pseudotyped viruses were generated by double transfection of HEK293T cells with a plasmid encoding a single round HIV clone (pNL4-3.tCD34.R-.E-, pOGH, pOGH-csGFP-only or pOGH-mKO2-only) together with a VSV-G protein encoding plasmid (pVSVG). In other experiments triple transfection was done with the transfer plasmid pHR-CMV-GFP-I-Sce1 together with the Δ8.91 packaging plasmid and pVSVG. Linear polyethylenimine (PEI; Polysciences) was used for plasmid transfections. Medium was replaced 6 h post transfection and supernatant collected after 72 h by filtration through a 0.22 μm pore membrane (Corning Inc.). The virus was concentrated using a Vivaspin 15–50 kDa cut-off column (Vivascience), DNase (Roche) treated and stored at −80 °C. The HR vectors were concentrated by 2 h of ultracentrifugation in a 20% sucrose cushion. Cells were seeded and infected for 3 days in 48-well plates (10% FCS, 0.01%

gentamicin RPMI) yielding an infection rate < 40% positive cells, as monitored by FACS analysis using a MACS Quant VYB FACS analyzer (Miltenyi Biotech GmbH), ensuring single-copy integration. Cells were washed twice in Phosphate Buffered Saline (PBS) 72 h post infection to remove residual virus and reseeded. FACS samples were taken every 2 days to monitor reporter gene expression. A SIV-based lentiviral vector carrying a spleen focus forming viral (SFFV) promoter driving a zeocin resistance gene and a LEDGF/p75 specific miRNA-based shRNA (Osório et al., 2014; Schrijvers et al., 2012a) was used to generate a SupT1 LEDGF/p75 knock down (KD) cell line. LEDGF/p75 depletion was monitored using Western blot and Q-PCR (>85% in SupT1 LEDGF/p75 KD cells, Supplementary Fig. 1a bottom panel). Nalm LEDGF/p75 control (+/c) and LEDGF/p75 KO cells (−/−) were generated previously and are described in (Schrijvers et al., 2012a).

2.2. Reporter Viruses

2.2.1. Multi-colored Reporter Vvirus (OGH)

A variant of the recently described LAI-based double reporter virus was used (Chavez et al., 2015), where a constitutive and a LTR-driven reporter are simultaneously measured to study the latent reservoir (Calvanese et al., 2013; Dahabieh et al., 2013). This orange-green HIV-1 (OGH) reporter virus variant encodes LTR-driven enhanced Green Fluorescent Protein (eGFP) in the *nef* gene position together with a constitutively active EF1alpha promoter driving mutant Kusabira-Orange2 (mKO2) expression instead of mCherry as described previously (Calvanese et al., 2013; Chavez et al., 2015) (Fig. 1a). An internal constitutive promoter driving mKO2 expression allows direct visualization of the LTR-silent latent proviral pool via the FACS measurement of mKO2-based red fluorescence.

2.2.2. HIV NL4-3.tCD34.R⁻.E⁻

HIV tCD34 is a NL4.3-based single round reporter virus containing the LTR driven truncated CD34 (tCD34) as a reporter protein in the *nef* gene position (Fig. 2a). We replaced the firefly luciferase gene in pNL4-3.Luc.R⁻.E⁻ (NIH aids reagent program) via *NotI–XhoI* digestion with a tCD34 cassette using standard PCR amplification methods. CD34 (cluster of differentiation 34) is a cell surface glycoprotein functioning as a cell-cell adhesion factor in HSCs but is not present on primary CD4⁺ T lymphocytes (Fehse et al., 2000). A truncated version was used to block signal transduction and expression was visualized using antibody-staining allowing for non-fluorescent based cell sorting. Human CD34-PE antibody (Miltenyi Biotec, Cat. No 130-081-002) was used to detect tCD34 expression.

2.3. Flow Cytometry Analysis

Prior to flow cytometry, cells were fixed for 15 min in 4% paraformaldehyde at room temperature. Expression of eGFP/mKO2 or tCD34 was monitored using a MACS Quant VYB FACS analyzer (Miltenyi Biotech GmbH) using a 488 nm, 50 mW DPSS (diode-pumped solid-state) and a 561 nm, 100 mW diode laser respectively and 525/50 nm–586/15 nm band pass filters. A total of at least 30,000 live cells were counted, as determined on the basis of forward scatter channel/side scatter channel (FSC-H/SSC-H) and doublets were excluded based on the FSC-A/FSC-H or SSC-A/SSC-H plot. Single reporter controls where used for compensation purposes. Data were analyzed using third party software (FlowJo).

2.4. Drug Treatment

The LEDGIN CX014442 (Christ et al., 2012) was added at different concentrations during single round infection and washed away together with residual virus 72 h post infection. Samples were harvested for FACS analysis and the remainder of infected cells was reseeded. FACS samples were taken every 2 days to monitor reporter gene expression. The

infected cells were reactivated from latency 11 days post infection using Tumor Necrosis Factor alpha (TNFα, 10 ng/mL, Immunosource), suberoylanilide hydroxamic acid (SAHA, 0.3 to 3 μM, AIDS reagents), Prostratin (5 μM, AIDS reagents) or phorbol 12-myristate 13-acetate (PMA, 0.3 μM, AIDS reagents) 24 h prior to analysis by flow cytometry. Time courses and drug concentrations are indicated in the individual experiments. LEDGINs were synthesized at Cistim/CD3 KU Leuven (courtesy of Dr. A. Marchand).

2.5. Genomic DNA Isolation and Quantification of Integrated Copy Number

Two million cells were pelleted and genomic DNA extracted using a mammalian genomic DNA miniprep kit (Sigma-Aldrich). Standard spectrophotometric methods were used to determine the genomic DNA concentration. Samples corresponding to 250 ng genomic DNA were used for analysis. Each reaction contained 12.5 μL iQ Supermix (Biorad), 40 nmol/L forward and reverse primer (5′ TGCACCCTGTGTCTCAACAT 3′ and 5′ GGCTTCAAGGTTGTCTCTGG 3′ respectively) and 40 nmol/L of tCD34 probe (5′ (6FAM)-GGCCACAACAAACATCACAG-(TAM) 3′) in a final volume of 25 μL. In all cases, RNaseP was used as an endogenous control for normalization (TaqMan RNaseP control reagent, Applied Biosystems, The Netherlands). Samples were run in triplicate for 3 min at 95 °C followed by 50 cycles of 10 s at 95 °C and 30 s at 55 °C in a LightCycler 480 (Roche-applied-science). Analysis was performed using the LightCycler 480 software.

2.6. Integration Site Amplification

Integration sites were determined as described previously (Marshall et al., 2007). In short, cells were seeded and transduced with a lentiviral vector for 3 days, then washed twice with PBS. Transduced cells were further cultivated for at least 10 days to eliminate non-integrated DNA. Cells were harvested and genomic DNA extracted using the GenElute Mammalian Genomic DNA miniprep kit (Sigma-Aldrich). Integration sites were amplified by linker-mediated PCR as described previously (Marshall et al., 2007). Genomic DNA was fragmented using MseI restriction digestion and linkers ligated. Provirus/host genome junctions were amplified by nested PCR using indexed primers. Products were gel-purified and sequenced using 454/Roche pyrosequencing (Titanium technology, Roche) on the 454 GS-FLX-instrument. Reads were filtered based on perfect matching of the LTR linker, barcode and flanking LTR. All sites were mapped to the human reference genome requiring a perfect match within 3 bp of the LTR end. Matched Random Control (MRC) sites were computationally generated and matched to experimental sites with respect to the distance to the nearest MseI cleavage site. Normalization of experimental HIV sites by the MRC sites corrects for the recovery bias due to cleavage by MseI. Analysis was performed as described previously (Marshall et al., 2007). A more detailed guide to the data presented can be found in (Ocwieja et al., 2011). Sequence logos were created using WebLogo 3.3 with compositional adjustment for the human genome base background distribution.

2.7. Single Cell Imaging of Proviral HIV (SCIP) Assay

20,000 U2OS cells/well were seeded in a 4 well chamber slides (Lab-TekTM) and transfected the next day with 200 ng of pCBASce plasmid encoding the I-Sce1 endonuclease using Effectene (Qiagen). Six hours post transfection cells were infected with 4 reverse transcriptase units (RTUs; SYBR Green-based Product Enhanced Reverse Transcriptase assay, SGPERT; (Pizzato et al., 2009) of the lentiviral vectors HR-CMV-GFP-I-SceI/VSV-G or HR CMV-GFP-I-Sce1-INA128T/E170G/VSV-G in Optimem medium containing 1% FCS for 2 h and fixed 48 h post infection with 4.0% paraformaldehyde in PBS for 5 min at room temperature (RT). After permeabilization with PBS containing 0.2% Triton-X100 for

10 min, samples were blocked overnight with 3% bovine serum albumin at 4 °C. The slides were incubated with the primary antibody directed against phosphorylated γH2AX (1:500, 05-636 Millipore) for 1 h at RT and with secondary fluorophore-conjugated antibodies for 1 h at RT. Slides were mounted with Vectashield mounting medium (Vector Laboratories). Nuclear fluorescent signal from γH2AX foci was acquired with the TCS SL laser-scanning confocal microscope (Leica Microsystems) equipped with galvanometric stage using a $63\times/1.4$ NA HCX PL APO oil immersion objective and processed by an image software (ImageJ, NIH.gov) (Di Primio et al., 2013). Background, i.e. spontaneous H2AX repair foci, were subtracted before further analysis as described in (Di Primio et al., 2013).

2.8. CD4^{+} T-cell Enrichment

Human peripheral blood mononuclear cells (PBMCs), obtained from the Red Cross Blood transfusion Center (Mechelen, Belgium) according to approved bioethical guidelines of our institute (S57175-IRB00002047), were purified from fresh buffy coats using lymphoprep density gradient centrifugation (Stem cell technologies). The CD4^{+} T cells were selectively enriched using Bi-specific MAb CD3.8 (0.5 μg/mL, AIDS reagents) for 5 days. Cells were cultured in RPMI 1640, 15% v/v FBS, 0.1% v/v Gentamicin, 100 U/mL IL-2 (Peprotech) (T-cell medium, TCM). Enriched total CD4^{+} primary T cells were infected with single round reporter virus for 2 h at 37 °C, washed twice in TCM and reseeded in medium containing different concentrations of LEDGIN CX014442. HIV infection was monitored 48 h post infection using flow cytometry analysis.

2.9. Reactivation of Latent Provirus in Primary CD4^{+} T-cells

Peripheral blood mononuclear cells (PBMCs) were isolated from fresh buffy coats obtained from the Red Cross Blood transfusion center (Mechelen, Belgium) according to approved bioethical guidelines of our institute (S57175-IRB00002047). Resting CD4^{+} T cells were purified using a custom-made EasySep negative selection kit (Stem Cell Technologies; 19052 cocktail, with the addition of CD25, CD69, and HLA-DR antibodies (catalogue number 19309VK)). The resulting 95% pure resting CD4 + T cells consisted of both naïve and central memory T cells (Sallusto et al., 1999). These freshly isolated resting CD4 + T cells were activated with 10 μg/mL PHA (Sigma-Aldrich) and 100 U/mL IL-2 (Peprotech) for 2 days before infecting with NL4.3 wt virus for 2 h (3.5×10^3 ng p24 per 1×10^7 cells/mL). Cells were washed twice with PBS and reseeded in the presence of varying concentrations of LEDGIN (CX014442) and 1 U/mL of IL-2. Four days post-infection cells were washed twice using PBS and some cells were harvested for quantification of integrated proviral DNA using real time PCR (nested Alu-LTR PCR, (Butler et al., 2001; Lewin et al., 2008) normalized for input DNA by qPCR for the CCR5 gene as previously described (Zhang et al., 1999). Other cells were reseeded in the presence of 10 nM PMA (Sigma-Aldrich) together with 10 μg/mL PHA (Sigma-Aldrich) or left untreated. PHA activated feeder peripheral blood mononuclear cells (PBMCs) were added 24 h after the activating stimulus to amplify virus replication and enhance detection of the infection (Saleh et al., 2011). Virus production was measured in culture supernatant at day 7 post-infection by p24 ELISA (Fujirebio Europe).

2.10. Statistical Analysis

Reactivation results are expressed as means ± standard error of the mean. Statistical analysis was assessed using multiple t tests and corrected using Sidak–Bonferroni with significance levels indicated. Ranked Wald statistics were used to calculate the statistical significance (asterisks) for a given genomic feature between integration site datasets relative to the DMSO treated condition (dashes). Significant deviation
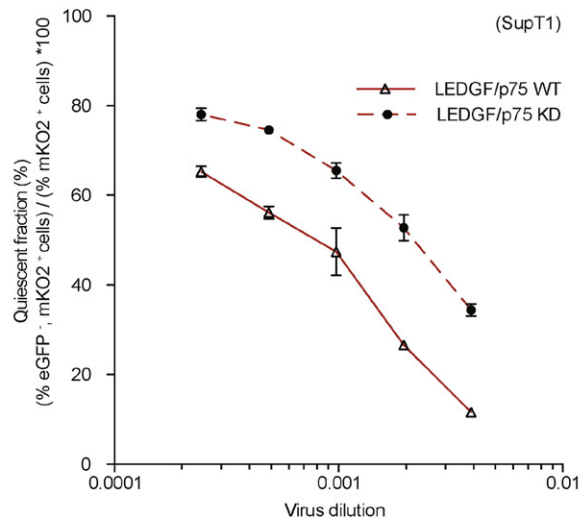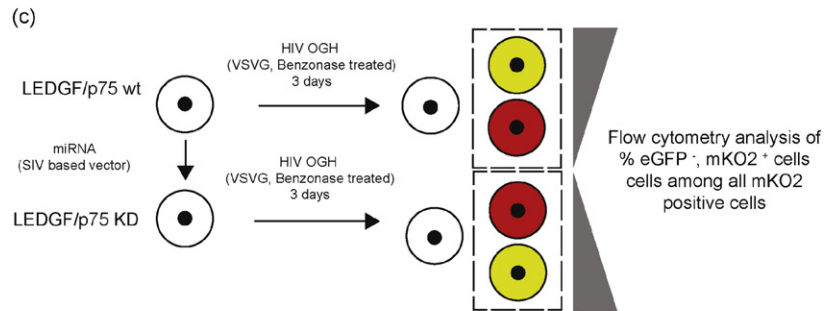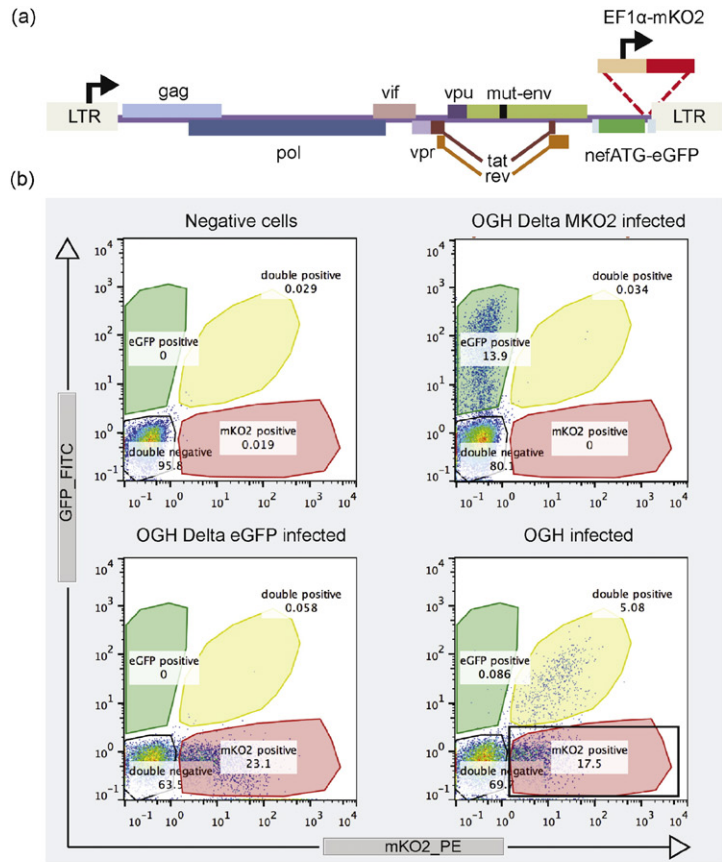
from the DMSO treated control dataset for safe harbor criteria was calculated using a Pearson's Chi-square test. ImageJ software was used to measure the relative distance of γH2AX foci to the nuclear rim. Statistical differences were calculated using a Kolmogorov–Smirnov test as described previously (Di Primio et al., 2013).

3. Results

3.1. LEDGF/p75 Depletion Results in a Quiescent Reservoir

We and others reported on retargeted proviral integration in LEDGF/p75-depleted cells (Ciuffi et al., 2005; Fadel et al., 2014; Schrijvers et al., 2012a; Shun et al., 2007). To study the role of LEDGF/p75 in establishing the latent reservoir, we used a variant of the recently developed double reporter virus that simultaneously measures a constitutive and a LTR-driven reporter (see the Materials and Methods section, Fig. 1a, (Calvanese et al., 2013; Chavez et al., 2015)). This orange-green HIV-1 (OGH) single-round reporter virus carries LTR-driven enhanced Green Fluorescent Protein (eGFP) together with a constitutively active EF1alpha promoter driving monomeric Kusabira-Orange2 (mKO2) expression (Fig. 1a). The double-fluorescent reporter virus allows quantification of distinct populations in the infected cell pool via FACS (Fig. 1b). Through the constitutively active EF1α promoter all infected cells express the mKO2 reporter. Provirus with an active LTR also expresses the eGFP reporter and is referred to as double positive, active virus, whereas provirus with a quiescent LTR does not express eGFP and is called here upon the quiescent provirus. Wild type and LEDGF/p75-depleted SupT1 cells (Supplementary Fig. 1a, bottom panel) were infected with a dilution series of single-round OGH virus. The percentage of infected cells was evaluated at three days post infection, discriminating productively infected cells (active provirus; eGFP$^+$, mKO2$^+$) from the latently infected populations (quiescent provirus; eGFP$^-$, mKO2$^+$). Single reporter constructs were used for validation (Fig. 1b). As expected, LEDGF/p75-depletion reduced HIV-1 infection 2- to 3-fold as judged by the percentage mKO2 positive cells (Supplementary Fig. 1a), in line with earlier data (Gijsbers et al., 2009; Schrijvers et al., 2012a; Vandekerckhove et al., 2006). Evaluation of the percentage of eGFP$^-$, mKO2$^+$ cells relative to the total number of infected cells (mKO2$^+$) provides an estimate of the fraction of quiescently infected cells in the infected pool (% eGFP$^-$, mKO2$^+$ cells) / (% mKO2$^+$ cells) $*$ 100. At all virus dilutions tested, LEDGF/p75 depleted cells contained more quiescent proviruses than WT cells (Fig. 1c). When this experiment was repeated in the Nalm$^{+/c}$ control and Nalm$^{-/-}$ LEDGF/p75 KO cell lines (Schrijvers et al., 2012a), similar effects were observed (Supplementary Fig. 1a, b). Since LEDGF/p75 depletion results in redistribution of HIV integration (Ciuffi et al., 2005; Fadel et al., 2014; Schrijvers et al., 2012a; Shun et al., 2007), these results suggest that the altered integration site distribution after LEDGF/p75 depletion increases the transcriptionally quiescent fraction.

3.2. LEDGF/p75 Depletion Decreases the Reactivation Potential of the Quiescent Reservoir

To further characterize the latently infected cell pool that is generated in LEDGF/p75-depleted cells, we set out to reactivate the latent provirus using different LRAs. Here, we used the LEDGF/p75 KO cell line (Nalm$^{-/-}$) to study whether latent provirus in LEDGF/p75-depleted cells has an altered reactivation potential. We made use of a NL4.3-based single reporter virus containing an LTR driven truncated CD34 (tCD34) as a reporter protein (NL4-3.tCD34.R-.E-/VSV-G, Fig. 2a).

Control (Nalm$^{+/c}$) and LEDGF/p75 KO (Nalm$^{-/-}$) cells were infected with a dilution series of HIV-tCD34. Virus dilutions were selected to result in equal integrated copy numbers, both the LEDGF/p75 control (Nalm$^{+/c}$) (1.45E−01 ± 1.40E−02 copies) and LEDGF/p75 KO (Nalm$^{-/-}$) cells (1.45E−01 ± 2.41E−02 copies) to compare the fold reactivation between both. Cells were reactivated 11 days post infection with different LRAs (Fig. 2b), and the fold reactivation (% tCD34) relative to DMSO between LEDGF/p75 WT and LEDGF/p75 KO conditions was measured 24 h later. The percentage of living cells amounted at least 75% of the total cell population in all conditions and was independent of LEDGF/p75 depletion (data not shown). Modest tCD34 reactivation was observed after addition of Phorbol Myristate Acetate (PMA) or Prostratin. An increase in the percentage tCD34 positive cells of 1.5–2 fold was observed for the Nalm$^{+/c}$ control while LEDGF/p75 KO (Nalm$^{-/-}$) conditions only experienced an increase of 1.3–1.5 fold when adding PMA (0.3–3 μM) or Prostratin (5 μM) (t-test with Sidak–Bonferroni correction; * $p < 0.05$, control compared to LEDGF/p75 KO). A similar effect was observed when stimulating with 1 μM Suberoylanilide Hydroxamic acid (SAHA). Yet, addition of 3 μM of SAHA resulted in a 3.2-fold reactivation of tCD34 in the presence of LEDGF/p75 but only a 2.2-fold reactivation in its absence (t-test with Sidak–Bonferroni correction; ** $p < 0.005$, WT compared to LEDGF/p75 KO) (Fig. 2b). Together, these data indicate that integration in the absence of LEDGF/p75 results in a larger quiescent cell pool upon infection (Fig. 1c) with a relatively larger proportion of cells refractory to reactivation (Fig. 2b).

3.3. LEDGIN Treatment Shifts HIV Integration Out of Transcription Units

Next, we evaluated the effect of recently developed LEDGINs, small molecules that inhibit LEDGF/p75–IN interaction and HIV integration (Christ et al., 2010; Demeulemeester et al., 2014a), on the HIV reservoir in cell culture. SupT1 cells were transduced with a single-round HIV-based lentiviral vector expressing eGFP in the presence of a dilution series of LEDGIN CX014442 (Christ et al., 2012). Flow cytometry and Q-PCR revealed a dose-dependent decrease in lentiviral transduction as represented by the % eGFP-positive cells and the number of integrated copies (Supplementary Fig. 2a and b). In a first step, we determined the distribution of HIV-based viral vector integration sites (Gijsbers et al., 2009; Marshall et al., 2007). The number of integration sites is indicated for each data set (Table 1, Fig. 3). We analyzed lentiviral integration frequencies relative to a set of genomic features (Table 1). In line with previous results, HIV integration in WT SupT1 cells was enriched in the body of genes (69.54% in RefSeq genes (Table 1)) disfavoring transcription start sites (TSS) and promoter regions (1.78% within 2 kb of the 5′ of a RefSeq gene and 2.02% within 2 kb of a CpG island) (Mitchell et al., 2004; Schroder et al., 2002). The integration sites shifted out of transcription units under LEDGIN-treatment (54.55% in RefSeq genes (50 μM); *** $p < 0.0001$, Chi-square test compared to DMSO) while integration close to TSS (6.94% (50 μM); *** $p < 0.0001$, Chi-square test compared to DMSO) and CpG islands (5.50% (50 μM); ** $p < 0.01$, Chi-square test compared to DMSO) increased in a dose-dependent manner. This shift in integration site distribution surpasses the one observed in LEDGF/p75-depleted cells (Ciuffi et al., 2005; Fadel et al., 2014; Schrijvers et al., 2012a; Shun et al., 2007). The fact that LEDGINs also inhibit the interaction between HRP-2 and HIV-1 IN (Schrijvers et al., 2012a), can explain this observation. Comparable data were observed for larger window sizes (2 kb and 4 kb are shown). Our results were corroborated in MT4 cells using multiple round (WT) HIV NL4-3 using the less potent

Fig. 1. LEDGF/p75 depletion increases the silent reservoir. (a) Schematic representation of the two-colored reporter virus carrying an eGFP driven by the viral LTR promoter in the Nef position and an entire constitutive transcriptional unit (EF1a-mKO2) inserted downstream. (b) Dot plots representing FACS analysis of SupT1 cells infected with the single reporter viral controls (OGH-Delta mKO2, OGH-Delta eGFP) or the double reporter virus OGH. The different cell populations are highlighted in the representative color. (c) LEDGF KD affects the fraction of silently infected fraction (% eGFP$^-$, mKO2$^+$ cells) / (% mKO2$^+$ cells) $*$ 100. Data represent averages of triplicates from a representative experiment and error bars indicate the standard deviation. All viruses are VSV-G pseudotyped. eGFP, Enhanced Green Fluorescent Protein; mKO2, Mutant Kusabira Orange 2.

LEDGIN CX05045 (Supplementary Table 1) (Christ et al., 2010). A genomic heat map comparing integration site data sets obtained in SupT1 LEDGF/p75 KD cells with WT SupT1 cells in the presence of various concentrations of LEDGIN is shown in Fig. 3. Analysis of global integration preferences clearly indicates a shifts out of transcriptionally active regions upon LEDGF/p75 KD (Fig. 3, compared to DMSO), in line with previously reported data (Gijsbers et al., 2009; Marshall et al., 2007; Shun et al., 2007). A similar shift was also observed under LEDGIN treatment at concentrations above 6 μM. In a more elaborate analysis we analyzed integration site frequencies relative to epigenetic features described in T cells (Supplementary Fig. 3b & c). Under WT conditions, HIV integration preferentially occurred near epigenetic markers associated with transcriptionally active regions (H3K4 mono-, di- and tri methylation, H3K14 and H4 acetylation, as well as acetylation or mono-methylation of H3K9/K27/K79, H4K20 and H2BK5, …) (De Ravin et al., 2014), while integration in transcriptionally silent regions or heterochromatin is disfavored (H3K27me3, H3K9me3 or H4K20me3 and

H3K79me3, respectively). The overall integration profile is closer to random upon addition of LEDGIN CX014442 (as shown by the decrease in color intensity towards black, cf. Color key Supplementary Fig. 3b and c). Supplementary Fig. 3c displays a more condensed heat map where epigenetic marks are grouped according to the respective chromatin states they associate with.

Since LEDGINs may potentially affect the inherent integration mechanism, resulting in aberrant integration or an altered local integration site preference, we evaluated sequence conservation and relative base frequency in the 18 bp genomic DNA sequence surrounding the integration sites (corresponding to the intasome footprint) using sequence logos (Supplementary Fig. 5). The WT local palindromic sequence logo surrounding the integration site (Holman and Coffin, 2005; Demeulemeester et al., 2014b)) was maintained in all conditions. In addition we calculated the percentage unique integration sites with an imperfect LTR chromosome junction relative to the total integration sites after LEDGIN
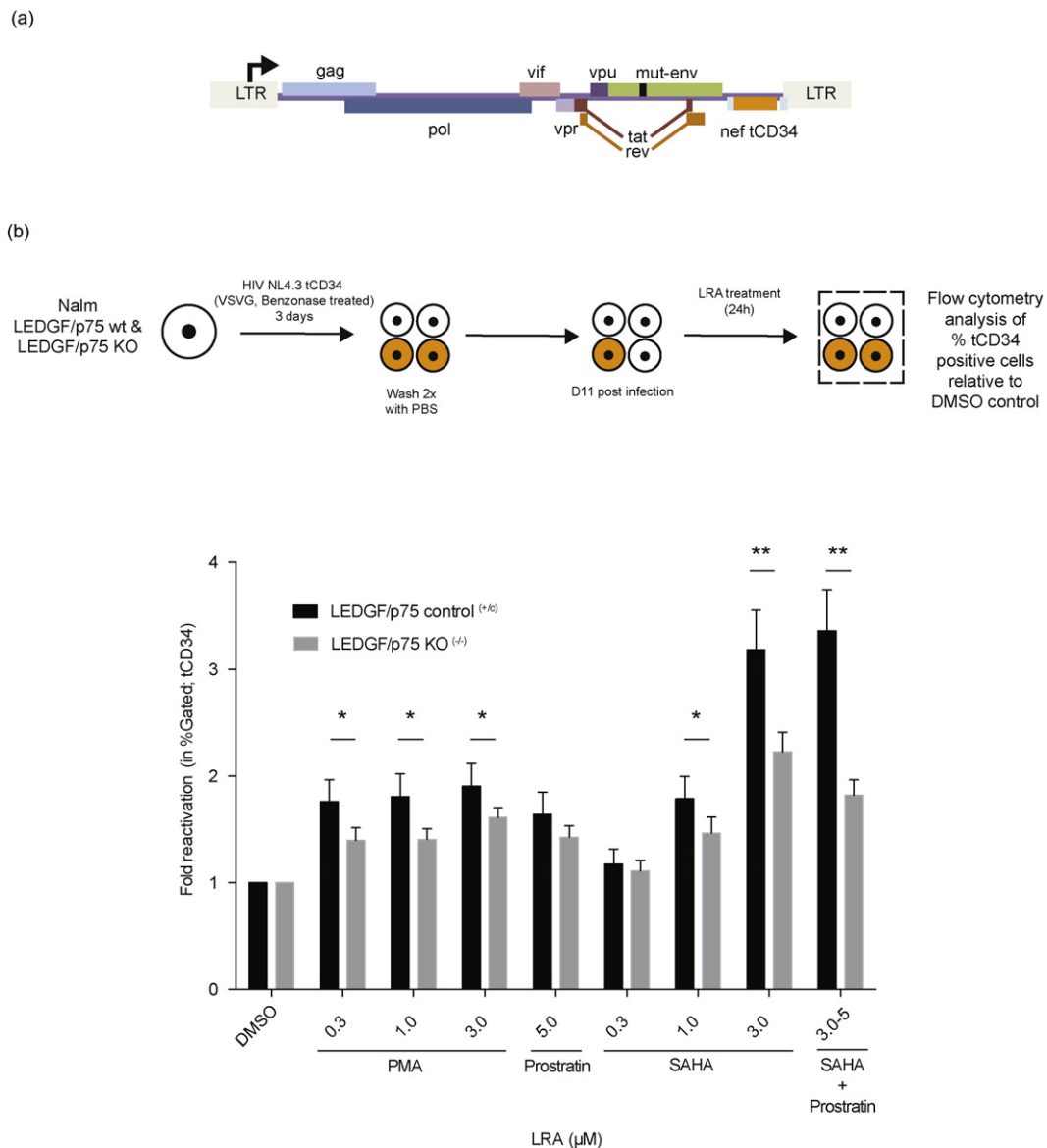

Fig. 2. LEDGF/p75 depletion reduces HIV reactivation from latency. (a) Schematic representation of the single round HIV reporter virus encoding a tCD34 driven by the viral LTR promoter in the nef position. (b) Bar diagram depicting the fold reactivation (as fold increase in % tCD34 positive cells). Nalm control (+/c) and Nalm LEDGF/p75 KO (−/−) cells were infected with a dilution series of single round reporter virus and the % tCD34 positive cells was monitored. 11 days post infection cells were reactivated using different LRAs at concentrations indicated. Data represent averages of 9 replicates from 3 independent experiments and error bars indicate the standard error of the mean (SEM). A statistical analysis was performed using multiple t tests and corrected using Sidak–Bonferroni (* $p < 0.05$, ** $p < 0.005$ vs. LEDGF/p75 KO) (SAHA; Suberoylanilide Hydroxamic Acid, PMA; Phorbol 12-Myristate 13-Acetate, Prostratin, DMSO; Dimethyl sulfoxide.). Normalization was based on equal integrated copy (IC) numbers. All viruses are VSV-G pseudotyped. tCD34; truncated Cluster of Differentiation 34.

Table 1

Integration frequency near mapped genomic features in the human genome. Table showing the percentage of HIV-based vector integration sites relative to features specific for integration such as integration into the body of genes (Refseq genes), TSS, CpG islands and DNase I-hypersensitive sites. 2 kb and 4 kb windows are shown (data are obtained from SupT1 cells). Colors depict the nature of the association based on the highest and lowest value in the column. Asterisks depict a significant deviation from the DMSO treated control dataset (two-tailed Chi-square test; *** p-values < 0.001); TSS, Transcription start sites; DHS, DNase I-hypersensitive sites.

Compound concentration (µM)	Type	Controls	TotalSites	InRefGene	% TSS within 2kb	% TSS within 4kb	% CpG within 2kb	% CpG within 4kb	% DHS within 2kb	% DHS within 4kb (SupT1)
DMSO ctrl	insertion	TRUE	3312	69.54	1.78	5.62	2.02	6.16	23.04	39.86
0.78125	insertion	FALSE	2451	70.58	2.00	5.92	2.33	5.83	24.07	39.94
1.5625	insertion	FALSE	2278	70.37	2.41	5.88	2.37	5.79	20.94	37.18
3.125	insertion	FALSE	2485	66.60	1.97	5.59	1.73	5.39	21.49	37.55
6.25	insertion	FALSE	3365	65.23**	3.03	6.45	2.97	6.39	21.78	37.12
12.5	insertion	FALSE	884	61.88***	3.96**	7.58**	3.39	7.35	23.64	38.57
25	insertion	FALSE	604	60.93***	4.30**	8.94**	4.97**	10.26	22.19**	40.07
50	insertion	FALSE	418	54.55***	6.94***	12.68***	5.50***	11.72	26.08***	40.67
DMSO ctrl	match	TRUE	9918	39.12	2.15	5.09	2.33	5.04	15.08	26.72
0.78125	match	FALSE	7341	39.71	1.98	4.41	2.38	4.62	15.79	27.23
1.5625	match	FALSE	6828	39.75	2.72	5.02	2.46	5.1	15.35	27.61
3.125	match	FALSE	7434	39.8	2.37	4.94	2.22	4.75	15.04	25.99
6.25	match	FALSE	10080	40.92	2.43	4.57	2.63	4.65	15.52	26.99
12.5	match	FALSE	2649	38.01	2.45	4.72	2.27	4.53	14.99	26.54
25	match	FALSE	1806	38.65	2.6	4.93	2.05	4.37	14.89	27.3
50	match	FALSE	1251	39.73	1.92	4.08	2.4	4.4	16.07	27.34

(CX014442) — insertion rows; (CX014442) — match rows

treatment (Supplementary Table 2 and Supplementary Fig. 6, Supplementary experimental procedures). Only a minor fraction (<2%) of the total integration sites was identified as containing imperfect LTR-chromosome junctions. We conclude that although LEDGINs retarget integration towards more random, residual integration events represent authentic integration without gross LTR deletions.

3.4. Abrogation of LEDGF/p75–IN Interaction Shifts 3D Localization of the Integrated Provirus Towards the Inner Nuclear Compartment

HIV-1 PICs and integrated HIV provirus preferentially localize in the nuclear periphery (Albanese et al., 2008; Di Primio et al., 2013; Francis et al., 2014). Recent reports associate preferential integration with nuclear import and distance to nuclear pore complexes (Lelek et al., 2015; Marini et al., 2015). Here we analyzed the 3D distribution of HIV-1 integrated provirus upon interruption of the LEDGF/p75–IN interaction. We first compared the distribution of HIV proviruses 48 h post infection in the Single Cell Imaging of Proviral HIV-1 assay (SCIP) (Di Primio et al., 2013) between LEDGF/p75 WT and LEDGF/p75 depleted U2OS cells (Fig. 4a). The distribution of integrated HIV provirus was analyzed by detection of γH2AX foci after I-Sce1 digestion (Fig. 4a). Twofold less integrants were detected after LEDGF/p75 depletion (Fig. 4a). Whereas in WT cells the viral genomes localized near the nuclear rim (Fig. 4b), the location of integrated provirus shifted towards the inner nuclear compartment after LEDGF/p75 depletion as indicated by the cumulative frequency plotted relative to the distance to the nuclear rim (Fig. 4b) confirming recent observations (Di Primio et al., 2013; Lelek et al., 2015; Marini et al., 2015). Since LEDGIN treatment shifts integration sites out of transcriptionally active regions comparable to LEDGF/p75 KD conditions (Fig. 3), we verified whether LEDGIN treatment might potentially affect the 3D-location of integrated provirus as well. Indeed, addition of 3 µM of LEDGIN CX05045 redistributed the integrated provirus towards the inner nuclear compartment. An HIV-1 mutant (HIV-IN-A128T/E170G), resistant to LEDGINs (Christ et al., 2010), was not redistributed (Fig. 4d). Therefore, these data demonstrate that LEDGF/p75 controls the nuclear topology of HIV-1 provirus and that LEDGINs may induce its spatial randomization.

3.5. The residual reservoir upon LEDGIN treatment is more quiescent

In a next step, we investigated whether LEDGIN-mediated retargeting also affected the quiescent reservoir, which would be in line with the effects demonstrated earlier in LEDGF/p75 depleted (KD/KO) cells. SupT1 cells were infected with the single-round OGH reporter virus in the presence of increasing concentrations of LEDGIN (CX014442). HIV OGH infection was measured 3 days post infection using flow cytometry resulting in the detection of cell populations carrying both productive (eGFP+, mKO2+ cells) and quiescent (eGFP−, mKO2+ cells) provirus (see also Fig. 1). LEDGIN treatment induced a dose-dependent decrease in the % of eGFP+, mKO2+ cells (Fig. 5a) as well as the overall mKO2+ cells (Fig. 5b). However, similar to LEDGF/p75 depletion (see Fig. 1c), LEDGIN treatment resulted in a relative increase of the quiescent fraction (% eGFP−, mKO2+ cells) / (% mKO2+ cells) ∗ 100 (Fig. 5c). No increase in the quiescent fraction was observed when adding increasing concentrations of the reverse transcriptase inhibitor AZT (data not shown) suggesting the phenotype was not merely due to inhibition of infection. Interestingly, nearly all infected cells were quiescent at 25 µM LEDGIN (CX014442). Several studies reported on the effect of integration orientation relative to endogenous genes on the HIV transcriptional state, with a possible enhancement of transcription when integrated in the same orientation or transcriptional interference when integrated in the opposite orientation. We therefore evaluated relative orientation frequencies of those integrations occurring within genes for the different integration site data sets (Supplementary Table 3). LEDGIN treatment resulted in a significant, dose-dependent increase in the fraction of integrations having an opposite orientation from 46.2%
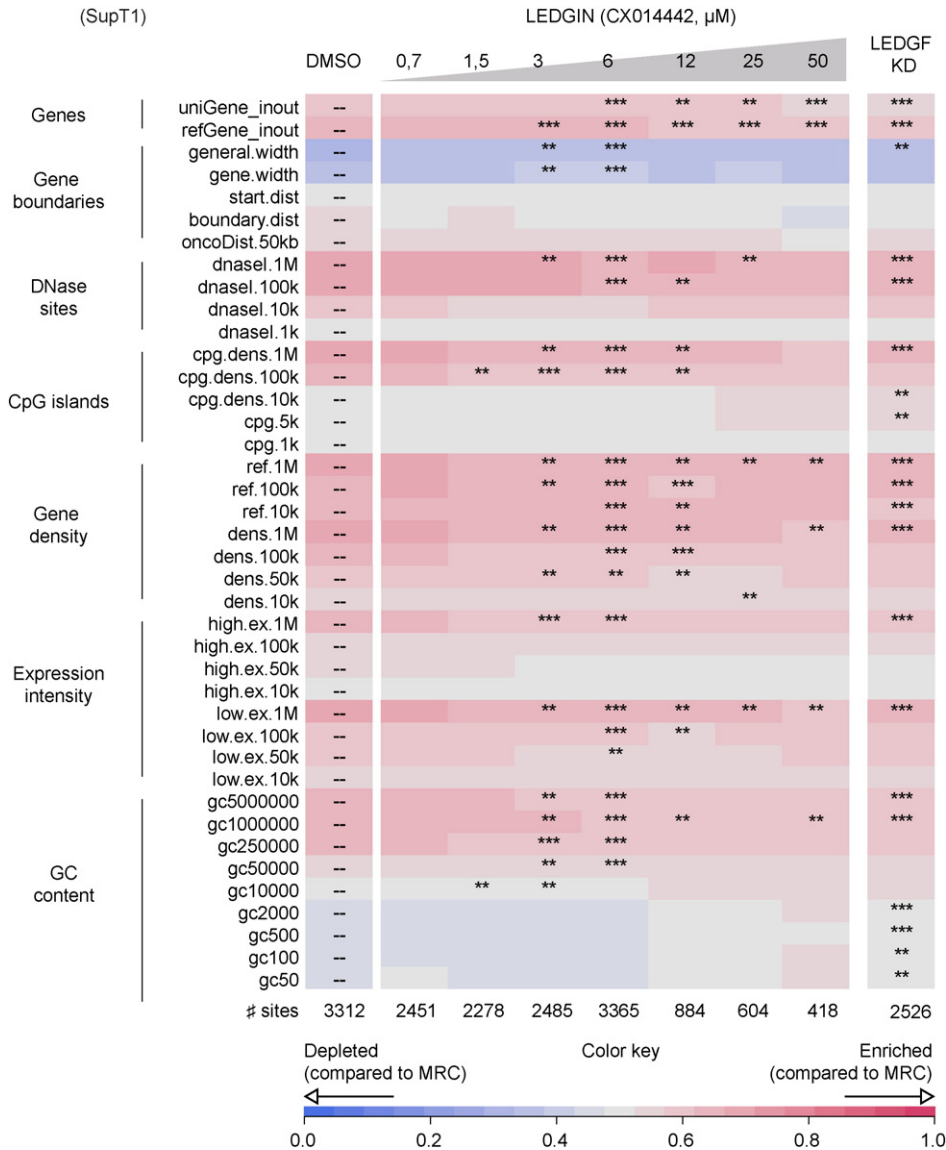
Fig. 3. LEDGIN inhibition of the LEDGF/p75–IN interaction retargets lentiviral integration. Integration site data sets obtained from SupT1 cells infected with LVP2A and treated with different concentrations of CX014442 (IC$_{50}$ CX014442 'early effect': 3.83 μM) were compared to different genomic features. A heat map was generated using the INSIPID software (Bushman Lab, University of Pennsylvania). Tile color depicting the nature of the correlation for an integration data set with the respective genomic/epigenetic feature (rows, left) relative to matched random controls, as indicated by the colored receiver operating characteristic (ROC) curve area scale at the bottom of the panel. Columns indicate different data sets. Statistical significance (asterisks, ranked Wald tests) is shown relative to the DMSO population (dashes). Significance is reached when $p < 0.001$, compared to the DMSO control (** $p < 0.01$; *** $p < 0.001$). CX014442 treatment during infection shows a dose dependent shift out of transcriptionally active regions. Lower significance is observed at the highest LEDGIN concentrations due to a lower copy number of integration sites (a more detailed guide to the data presented can be found in Ocwieja et al., 2011).

to 56.7% (p-value < 0.005, Pearson's Chi-square compared to the DMSO control condition) with respect to the targeted gene.

3.6. LEDGIN Treatment Results in a Quiescent Reservoir Resistant to HIV Reactivation

Next we studied whether LEDGIN treatment also reduces the reactivation potential after reporter gene silencing, as observed under LEDGF/p75 depletion (Fig. 2). The LEDGIN-induced increase in the silent reservoir, together with the reduced HIV reactivation potential could hold promise to reduce the functional reservoir. SupT1 cells were infected with single round HIV-OGH double reporter virus (Fig. 6) or HIV-tCD$_{34}$ (Supplementary Fig. 4) under varying LEDGIN (CX014442) concentrations and reactivated with LRAs. To demonstrate that LEDGIN-retargeted provirus remains refractory to general cell activation TNFα was used as a reactivation agent. Data depict a representative virus dilution. In Fig. 6a the percentage of eGFP$^+$, mKO2$^+$ cells and overall %

mKO2$^+$ positive cells is plotted after stimulation with DMSO or TNFα for 24 h (open squares and open triangles, for TNFα and DMSO, respectively). Stimulation with TNFα did not affect the percentage living cells (>85% in all conditions) neither in the absence or presence of LEDGIN (data not shown). The % eGFP$^+$, mKO2$^+$ positive cells are significantly higher after stimulation with TNFα compared to DMSO at the different LEDGIN concentrations, while the overall percentages of mKO2$^+$ positive cells remain constant (compare red and green lines). LEDGIN treatment resulted in reduced reactivation as measured by the fold increase of productively infected cells (% eGFP$^+$, mKO2$^+$) in a concentration-dependent manner, with 25 μM CX014442 reducing the reactivation by TNFα 2-fold (Fig. 6b). A slope of -0.034 ± 0.009 fold/μM was calculated using a linear regression model (significant deviation from zero; $p < 0.0018$, Fig. 6b). On the other hand, increasing concentrations of LEDGIN CX014442 antagonized the reactivation potential of the latently infected pool as represented by the decrease the fraction of quiescent cells (% eGFP$^-$, mKO2$^+$ cells) / (% mKO2$^+$ cells) ∗ 100 (Fig. 6c). A
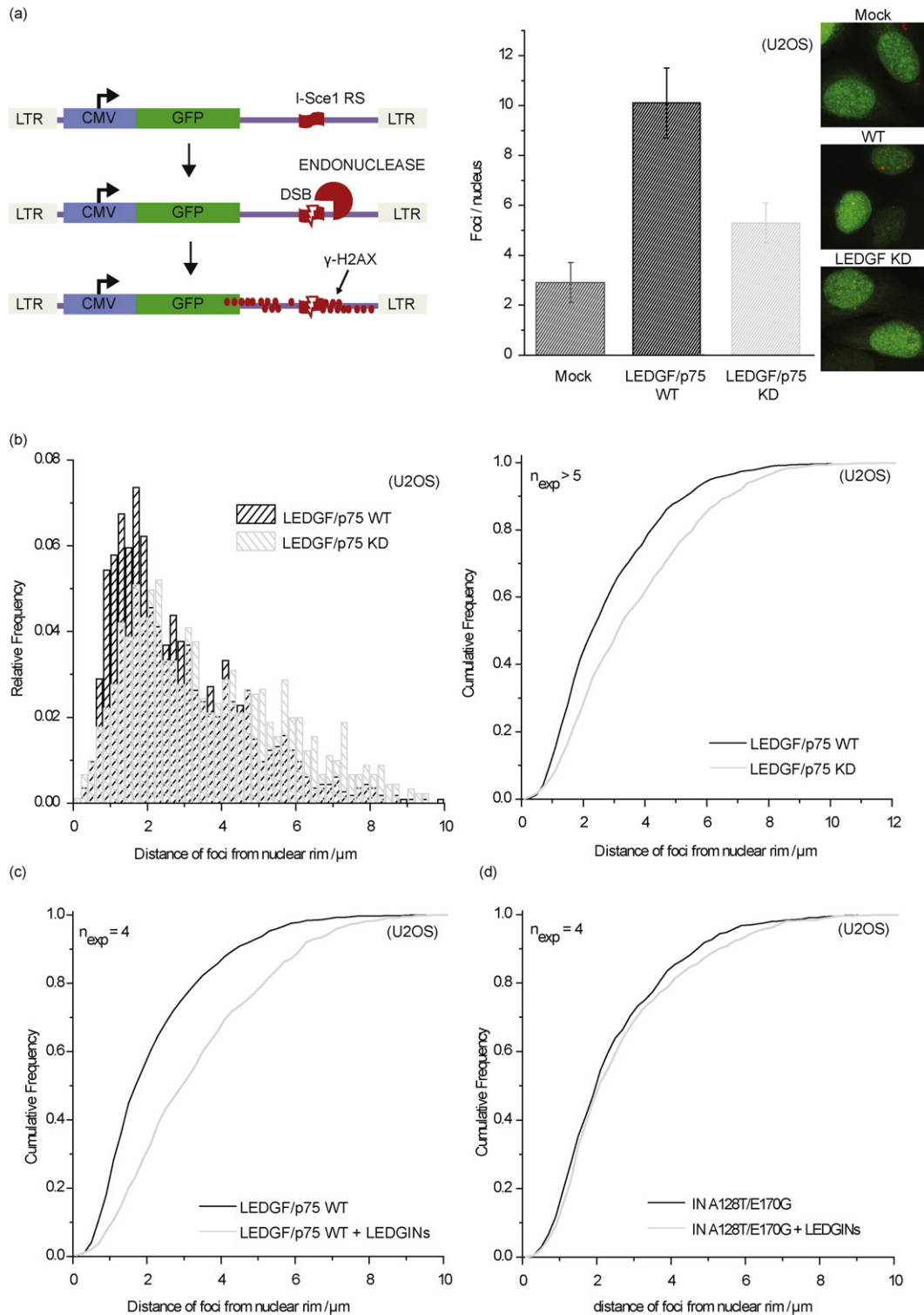
Fig. 4. LEDGIN treatment shifts HIV-1 proviral localization towards the inner nuclear compartment. U2OS WT or LEDGF/p75 depleted cells were infected with a HIV derived vector pHR-CMV-EGFP with or without an I-SceI site (mock) and γH2AX foci quantified per nucleus 48 h post infection after endonuclease digestion. (a) SCIP analysis of proviral DNA corresponding to γH2AX foci (red) in U2OS cells. Bar diagram in the right panel depicts the number of proviruses (H2Aγ foci) detected under each condition. Error bars represent standard deviations from at least three experiments. (b) 3D nuclear localization of HIV-1 provirus relative to the nuclear rim in LEDGF/p75 KD (empty bars) or WT U2OS cells (grey bars) ($p < 0.001$, Kolmogorov–Smirnov test) ($n = 1000$). The right panel depicts the cumulative frequency for the distance relative to the nuclear rim. (c) Cumulative frequency of the 3D nuclear localization of HIV-1 provirus relative to the nuclear rim in U2OS cells treated (grey) with or without (black) 3 μM of LEDGIN CX05045 ($p < 0.001$, Kolmogorov–Smirnov test) ($n = 650$). (d) Cumulative frequency of the 3D nuclear localization of HIV-1 provirus relative to the nuclear rim in U2OS cells infected with the HIV-1 INA128T/E170G and treated with (grey) or without LEDGINs (black, CX05045, 3 μM, $4 \times IC_{50}$) ($p > 0.05$, Kolmogorov–Smirnov test) ($n = 650$). Number of experiments is indicated in each plot (>100 cells counted/experiment).
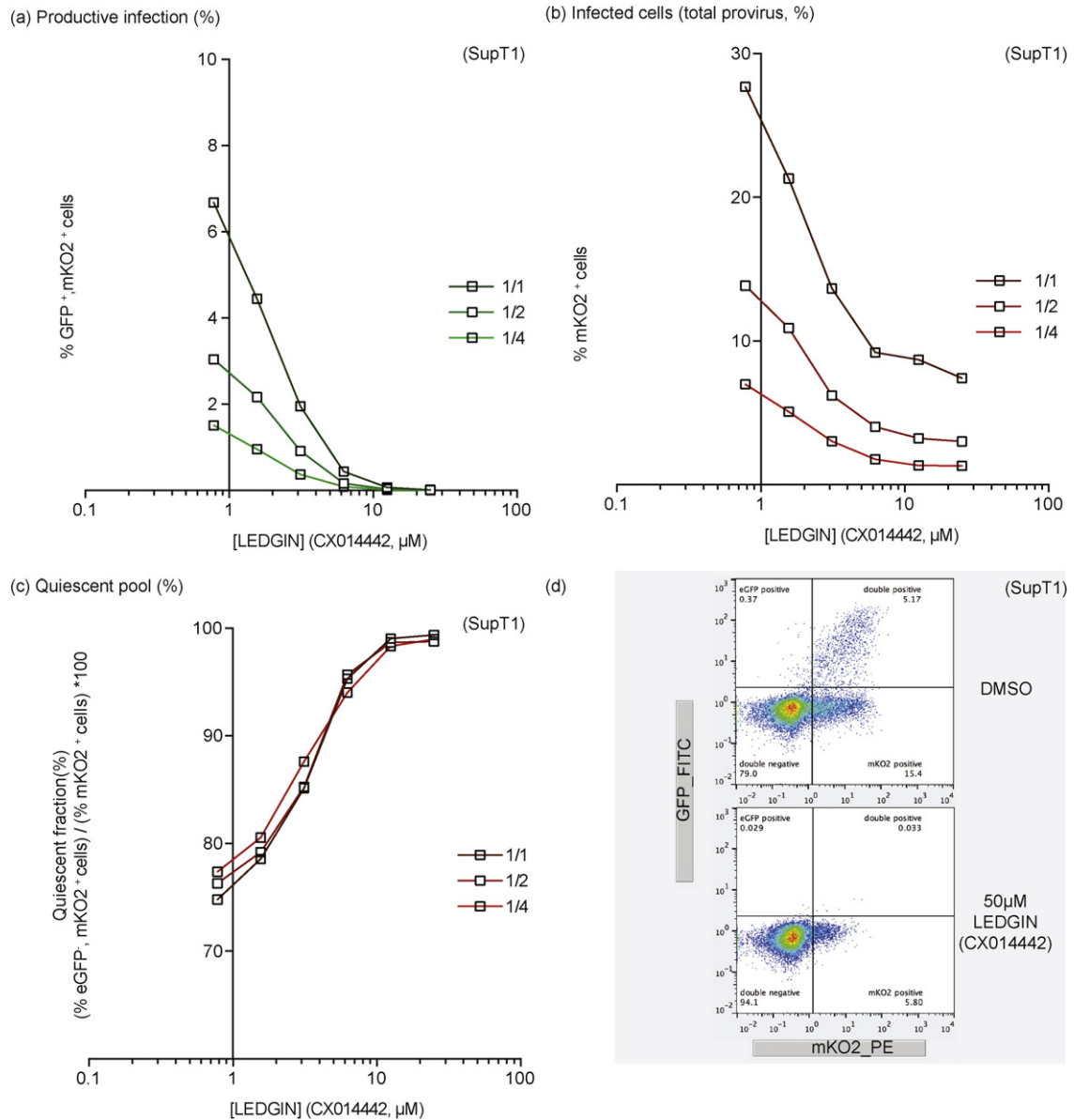
Fig. 5. LEDGIN-mediated retargeting of integration increases the quiescent reservoir. SupT1 cells were infected with three different dilutions of HIV OGH (a) Dose–response curve showing a decrease in % eGFP$^+$, mKO2$^+$ cells with increasing LEDGIN concentration. Three different virus concentrations are depicted in green. (b) Dose–response curve showing a decrease in the overall % mKO2$^+$ cells with increasing LEDGIN concentration. Three different virus concentrations are depicted in red. (c) The fraction of quiescent cells (% eGFP$^-$, mKO2$^+$ cells) / (% mKO2$^+$ cells) * 100 increases upon addition of LEDGINs. Three different vector dilutions are depicted in red. All viruses are VSV-G pseudotyped. (d) Representative dot plots depicting the different cell populations under two different conditions, numbers in the quadrant indicate the percentage of cells. All vectors are VSV-G pseudotyped. eGFP, Enhanced Green Fluorescent Protein; mKO2, Mutant Kusubira Orange 2.

slope of $-0.93 \pm 0.08\%/\mu M$ was calculated using a linear regression model (significant deviation from zero; $p < 0.0001$, Fig. 6c). Similar results were observed for HIV-tCD$_{34}$ where LEDGIN (CX014442) treatment resulted in a dose-dependent inhibition of reactivation from latency (reactivation IC$_{50} \approx 7.24\,\mu M$) as evidenced by the reduced increase in the % tCD34 positive cells (Supplementary Fig. 4a & b). This inhibition of reactivation was seen with various LRAs (Supplementary Fig. 4c). Raltegravir treatment did not result in this phenotype (Supplementary Fig. 4c & d), excluding integration inhibition as such or an increase in non-integrated 2-LTR circles as the cause of this effect. In conclusion, LEDGIN treatment reduces the reactivation potential of the quiescent HIV pool.

3.7. LEDGIN Treatment Retargets HIV Integration Into Safer Locations

The strategy to push HIV into latency by retargeting provirus integration away from active transcription units due to uncoupling of the LEDGF/p75–IN interaction may be associated with an altered risk of insertional mutagenesis. Insertional mutagenesis due to deregulation of neighboring gene expression is a concern in gene therapy applications with lentiviral vectors (Cavazzana-Calvo et al., 2010). In addition, two studies revealed the existence of clonally expanded CD4$^+$ cell populations carrying integrated HIV provirus in HIV-1 patients on prolonged antiretroviral therapy (Maldarelli et al., 2014; Wagner et al., 2014). Therefore we evaluated whether the residual integration profile under LEDGIN treatment has a different "safety" profile using stringent criteria used in gene therapeutic applications (Papapetrou et al., 2011). We investigated following criteria defining potentially unsafe integration events: integration near transcription start sites (<50 kb), oncogenes (<300 kb) or miRNA coding regions (<300 kb) and integration into transcription units and ultraconserved elements (UCR). Integration events occurring outside these features are considered to be safe (Table 2) (Papapetrou et al., 2011). For each data set, we calculated

the percentage of potentially unsafe integration sites according to a given criterion (Table 2) and determined the final percentage of safe sites (positioning outside these regions). The most pronounced and dose dependent decrease was observed for integrations falling within

transcription units. For the calculation of the final % safe-sites all 5 criteria were taken into account and the risk analysis is therefore affected by the different parameters. In the parental SupT1 cell line only 10.7% of all vector integration sites can be considered safe in
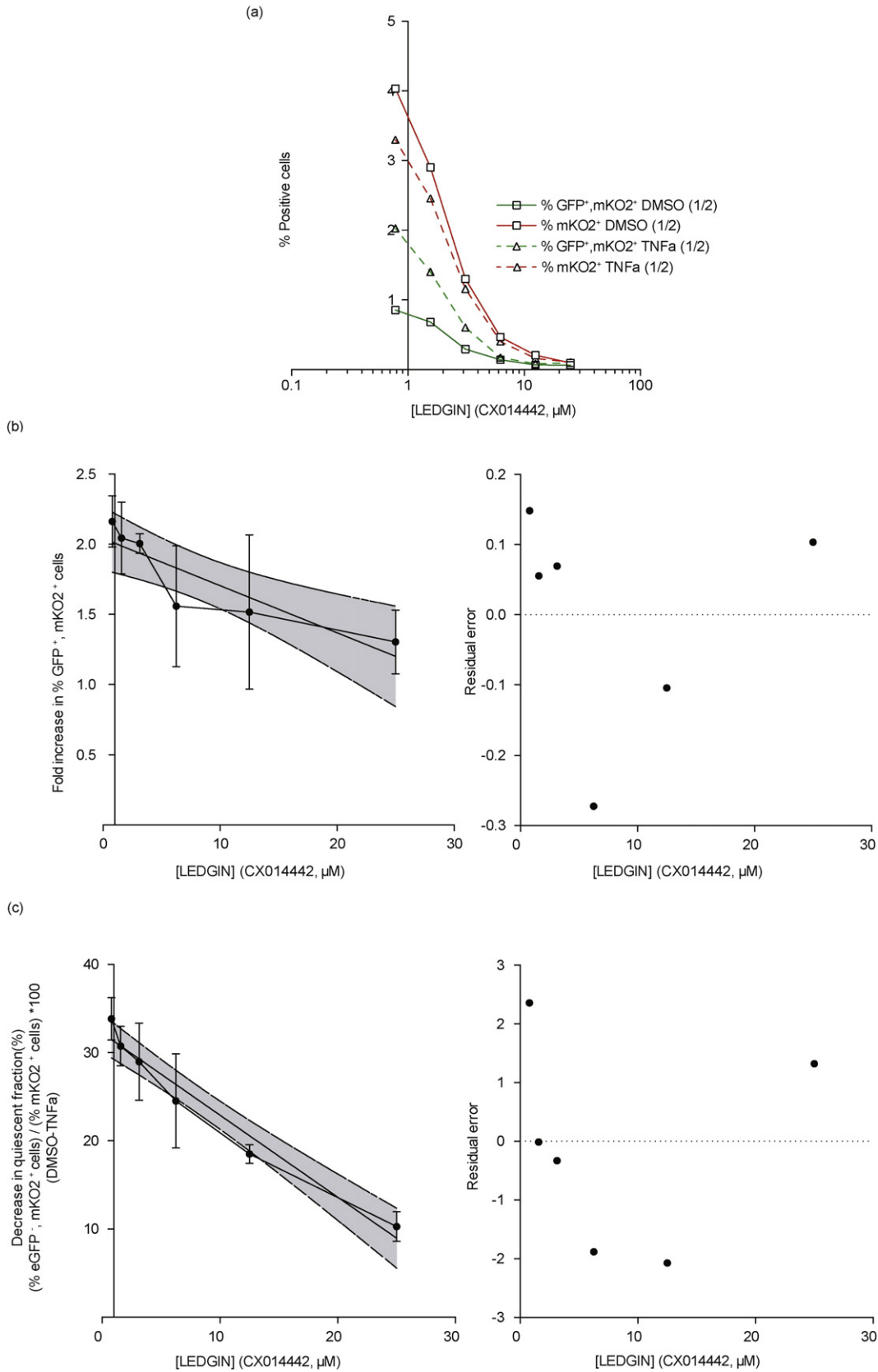
comparison to 28.5% for the matched random control datasets (MRC). LEDGF/p75 depletion increased the percentage safe sites to 14.7% (p-value < 0.005, Pearson's Chi-square compared to the DMSO control condition), a phenotype that is reverted upon LEDGF/p75 back complementation (data not shown). The shift in integration site distribution under LEDGIN treatment (Fig. 3, Supplementary Fig. 3a–c), coincides with a dose-dependent increase in percentage of safe integrations (16.51% at 50 μM, p-value < 0.005, Pearson's Chi-square compared to the DMSO control condition), consistent with the data obtained under LEDGF/p75 depletion.

3.8. LEDGIN Treatment Inhibits Integration, Relatively Increases the Quiescent Viral Reservoir and Reduces Reactivation in Primary CD4+ T Cells

Since recent studies reported the existence of a latently infected cell population after infection of activated primary CD4+ T cells (Calvanese et al., 2013; Chavez et al., 2015; Dahabieh et al., 2013), we tried to corroborate the effect of LEDGIN treatment on proviral latency in this model. Human PBMCs were purified, selectively enriched for CD4+ T cells using Bi-specific MAb CD3.8 and infected with the OGH reporter virus, in the presence or absence of LEDGINs (Fig. 7a,b). Similar to the results observed in SupT1 cells, LEDGIN (CX014442) treatment induced a dose-dependent decrease in the % infected cells (decrease in % eGFP+/mKO2+ cells or overall % mKO2+ cells, Fig. 7a) and an increase in the fraction quiescent cells (% eGFP−, mKO2+ cells) / (% mKO2+ cells) ∗ 100 (Fig. 7b) reaching 46.3% quiescence at a CX014442 concentration of 25 μM (representative data from one donor are shown for 2 different donors tested). Next we evaluated the multimodal effect of LEDGIN treatment on integration, assembly and reactivation in a multiple round reactivation model using WT HIV in resting CD4+ T-cells in order to model the in vivo situation. PHA/IL-2 activated primary (resting) CD4+ T cells were infected with NL4.3 virus in the presence of submicromolar concentrations of LEDGINs. At day four post infection (p.i.) LEDGINs were removed and cells were reseeded in the presence of PMA and PHA. Virus production upon reactivation was measured at day 7 p.i. by p24 ELISA. LEDGIN treatment reduced the number of proviral DNA copies in CD4+ T-cells in a dose-dependent manner (Fig. 7c). These residual integrants were less susceptible to reactivation as displayed by the reduced p24 production (Fig. 7d, data show the average for two different donors tested). Apart from reducing overall integration, these data suggested that LEDGIN treatment during HIV infection leads to quiescence of the residual integrants both in SupT1 and primary CD4+ T-cells. This quiescent reservoir appears less susceptible to reactivation.

4. Discussion

The moral duty to respond to the call for an HIV cure calls for exploration of experimental and innovative HIV cure strategies. As a complement to current purge-and-kill approaches aimed at forcing HIV out of its hiding places to obtain a sterilizing cure, we here provide experimental evidence for a strategy to push the virus towards transcriptional quiescence by interference with LEDGF/p75, the main determinant of integration site selection. General belief states that latency is an accident rather than a default pathway of an actively replicating cytopathic virus. The fact that LEDGF/p75, the tethering determinant of HIV integration, directs integration preferentially towards actively transcribed regions, ensuring productive infection, is consistent with this notion. Recently, it was proposed that HIV latency is a hardwired, evolutionarily conserved switch increasing the likelihood of successful mucosal transmission during primary infection (Razooky et al., 2015; Rouzine et al., 2015). Whereas HIV Tat is known to be the main viral determinant in controlling the HIV transcriptional state, the contribution of other viral and host determinants to the transcriptional state of the HIV provirus awaits further clarification. Here we investigated the role of LEDGF/p75 in the establishment of HIV latency. We demonstrate that LEDGF/p75 depletion, known to result in retargeting of integration away from the body of actively transcribed genes (Fadel et al., 2014; Schrijvers et al., 2012a; Shun et al., 2007), increases the fraction of quiescently infected cells and simultaneously decreases the reactivation potential of the proviruses. In light of the recently proposed role of LEDGF/p75 (and the Iws1/Spt6 complex) in post-integration HIV transcriptional repression (Gérard et al., 2015), this observed decrease may even be an underestimation of the contribution of the integration environment to the latent phenotype. Taken together, these observations suggest that disruption of the LEDGF/p75–IN interaction not only inhibits integration but could as well affect the establishment of the latent pool and the reactivation from latency.

Recently developed LEDGINs, small molecule inhibitors of LEDGF/p75–IN interaction, allowed us to test this hypothesis. Indeed here we demonstrate: (i) a LEDGIN-mediated shift in lentiviral integration site distribution resembling LEDGF/p75 depletion (out of the body of actively transcribed genes, with increased integration in the vicinity of CpG islands) ii) strongly reduced but authentic residual integration, (iii) a LEDGIN-mediated shift in 3D nuclear location of HIV provirus away from the nuclear rim; (iv) a relative increase in the fraction of quiescent proviruses and (v) a dose-dependent block in HIV reactivation from latency both in cell lines and primary CD4+ T-cells. It was recently proposed that pushing enough proviruses into quiescence could drive the basic reproduction number of HIV below 1, resulting in unsustainable infection (Rouzine et al., 2015). LEDGIN treatment apparently succeeds in rendering (almost) 100% of the virus into a quiescent state refractory to reactivation (Figs. 5c & f and 6). Although final proof will only be obtained in clinical trials, our cell culture data in relevant cell lines and primary cells provide evidence for the feasibility of this strategy. The importance of the site of integration in the human genome for basal transcriptional activity of HIV was evidenced more than a decade ago (Jordan et al., 2001). Now it is known that genomic target site selection during lentiviral integration is a multi-step process where biases are introduced at different levels, which each in part affect the stochastic proviral gene expression levels. At least three levels can be recognized. First, nuclear topology and proximity to the nucleopore affect integration site selection (Di Primio et al., 2013; Marini et al., 2015). Next, chromatin readers such as LEDGF/p75 or HRP-2 that recognize epigenetic marks associated with transcriptional activity tether the preintegration complex to active gene regions. No data exist suggesting a protein gradient. Therefore, as proposed by Marini et al. (2015), preferential lentiviral integration within the proximity of the nuclear periphery probably reflects the encounter by the HIV PIC of the first LEDGF/p75 bound

Fig. 6. LEDGIN treatment reduces reactivation from latency. SupT1 cells were infected with single round double reporter virus (OGH) and treated with different concentrations of CX014442 (as indicated). % eGFP–% mKO2 positive cells were monitored, respectively. 11 days post infection cells were reactivated using TNFα (10 ng/mL). (a) Dose–response curve showing the % eGFP+, mKO2+ cells and the overall % mKO2+ cells after reactivation with DMSO or TNFα. (b) Average fold increase in percentage eGFP+, mKO2+ or productively infected cells upon stimulation with TNF alpha relative to the DMSO treated condition. (c) Average decrease in the fraction quiescent cells (% eGFP−, mKO2+ cells) / (% mKO2+ cells) ∗ 100 or silent reservoir fraction upon stimulation with TNF α relative to the DMSO treated condition. Data in (b) and (c) represent averages of 3 different vector dilutions and error bars indicate the standard deviation. The straight lines represent the linear regression calculations together with the 95% confidence band plotted in grey and the residual error relative to the linear regression plot is depicted in the right panel. TNFα; Tumor Necrosis Factor alpha, DMSO; Dimethyl sulfoxide, eGFP; Enhanced Green Fluorescent Protein, mKO2; Mutant Kusubira Orange 2, All viruses are VSV-G pseudotyped.

Table 2

Integration frequency near safe harbor criteria. Table showing the percentage of HIV-based vector integration sites relative to features used to define UNsafe harbors. These criteria are considered to be UNsafe: TSS, Oncogenes, miRNA encoding regions, Transcription units and ultra-conserved regions. The % integrations negatively associated with these 5 features is used to calculate a safety profile. Colors depict the nature of the association based on the highest and lowest value in the column. Asterisks depict a significant deviation from the DMSO treated control dataset (Pearson's Chi-square test; ***, p-values <0.005; **, p-values <0.05; *, p-values < 0.5).TSS, Transcription start sites; UCR, Ultra conserved regions.

(SupT1)

|	Compound concentration (µM)	Type	Controls	total.sites	% within 50kb of TSS		% within 300kb of onco		% within 300kb of miRNAs		% in transcript. Units		% in UCR		Total % safe	
(CX014442)	DMSO Ctrl	insertion	TRUE	3312	32.04		37.71		25.88		74.68		7.29		10.24	
	0.78125	insertion	FALSE	2451	31.13	*	38.15		25.54		74.95		6.36	*	11.14	
	1.5625	insertion	FALSE	2278	29.28	**	35.47	*	22.52	***	75.11		7.24		10.36	
	3.125	insertion	FALSE	2485	28.57	***	35.45	*	23.34	**	71.91	**	7.77	*	11.31	*
	6.25	insertion	FALSE	3365	29.46	**	33.03	***	21.76	***	70.48	***	6.03	*	13.32	***
	12.5	insertion	FALSE	884	31.33		33.03	**	24.89	*	67.42	***	9.39	**	13.24	**
	25	insertion	FALSE	604	29.80	*	35.26	*	21.52	**	66.06	***	6.95	*	14.57	**
	50	insertion	FALSE	418	32.54		35.65		22.25	*	59.57	***	5.98	*	16.51	***
	LEDGF/p75 KD	insertion	TRUE	4664	32.22		36.16	*	21.67	***	64.96	***	6.72	*	14.71	***
(CX014442)	DMSO Ctrl	match	FALSE	9918	24.16		23.36		14.90		45.07		5.21		29.39	
	0.78125	match	FALSE	7341	24.51		24.55		14.93		45.52		5.38		28.46	
	1.5625	match	FALSE	6828	25.47		23.68		15.39		46.16		5.40		28.31	
	3.125	match	FALSE	7434	23.57		23.92		15.15		46.12		4.94		28.90	
	6.25	match	FALSE	10080	23.96		23.56		15.51		47.10		5.03		28.52	
	12.5	match	FALSE	2649	24.31		24.73		14.65		44.62		5.21		29.26	
	25	match	FALSE	1806	23.32		21.99		15.35		44.76		5.32		29.42	
	50	match	FALSE	1251	25.90		24.62		15.11		46.92		5.28		26.62	
	LEDGF/p75 KD	match	FALSE	13961	24.25		24.12		14.83		46.32		5.41		28.66	

(a) Productive infection (%)

(b) Quiescent pool (%)
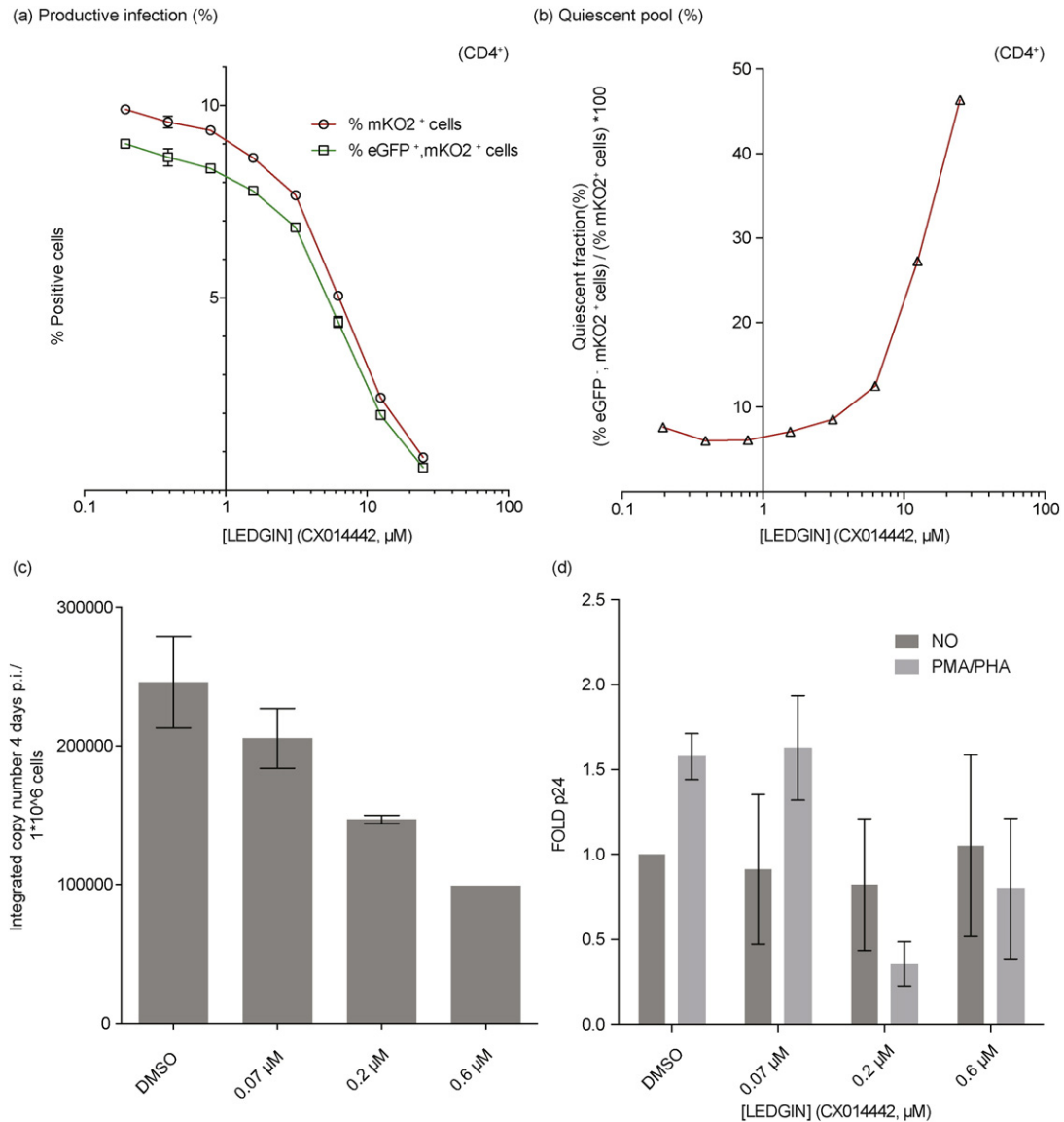
Fig. 7. LEDGIN treatment inhibits integration, induces quiescence of the residual viral reservoir and reduces reactivation in primary CD4$^+$ T cells. (a) Activated CD4$^+$ T-cells were infected with single round double reporter virus (OGH) and the % eGFP and % mKO2 positive cells were monitored. Dose–response curve shows a decrease both in the % eGFP$^+$, mKO2$^+$ cells and overall % mKO2$^+$ cells with increasing LEDGIN (CX014442) concentration. (b) The fraction of silently infected cell population (% eGFP$^-$, mKO2$^+$ cells) / (% mKO2$^+$ cells) $*$ 100 increases upon addition of LEDGINs. Data are representative for two different donors. All vectors are VSV-G pseudotyped. eGFP, Enhanced Green Fluorescent Protein; mKO2, Mutant Kusubira Orange 2. (c) Activated CD4$^+$ T-cells were infected with NL4.3 virus under different LEDGIN concentrations. 4 days p.i. integrated copy numbers were determined using a quantitative Alu-LTR PCR. (d) 4 days p.i. CD4$^+$ T-cells were reactivated using PMA/PHA and p24 production in the supernatant was monitored 7 days p.i. by ELISA. Data from show the average for two different donors tested $\pm$ SEM. PHA, phytohaemagglutinin; PMA, phorbol 12-myristate 13-acetate.

chromatin close to nucleopores. Finally, bias for target DNA base recognition by integrases also influences local and global integration patterns (Demeulemeester et al., 2014b, 2015; Serrao et al., 2015). In theory, interference with any of those mechanisms could shift the resulting proviral reservoir from transcriptionally active to quiescent. Both LEDGF/p75 depletion and LEDGIN treatment affect integration, integration site selection (Fig. 3, Supplementary Fig. 3a–c) and nuclear location (Fig. 4). Probably the reduced reactivation due to altered chromatin context is not entirely reflected by the features measured in the integration site analysis. As shown, aberrant integrations or LTR deletions are most likely not contributing, or only to a minor extent (Supplementary Fig. 5 and Table 2). In the absence of LEDGF/p75, HRP2 determines HIV integration site selection. The fact that LEDGINs also inhibit the interaction between HRP-2 and HIV-1 IN (Schrijvers et al., 2012a), can explain the more pronounced effect of LEDGINs on reactivation from quiescence compared to LEDGF/p75-depletion. Identification of the exact nature of

the altered chromatin context responsible for the observed phenotype awaits further experimentation. HIV latency is of multifactorial nature and the transcriptional state of integrated provirus is not only influenced by molecular determinants but also depends on the infected host cell and its activation state (Dahabieh et al., 2015). Therefore the respective quiescent fraction and responsiveness to different LRAs might alter depending on the cell model used since promoter activity may differ between cell types. In order to study the effect of integration site distribution on HIV latency we used NL4.3-based (HIV-tCD34) and LAI-based (OGH) single round reporter viruses in a concise reactivation setup in T-cell lines and activated CD4$^+$ T-cells. LEDGINs block HIV replication during integration (referred to as 'the early effect') as well as during assembly (i.e. 'the late effect'), with inhibition during the late step having a 10- to 100 fold higher potency than the early step (Debyser et al., 2015). In the experiments with single round virus, we used micromolar concentrations of LEDGIN, required to inhibit the

early step. Interestingly, recent experimental results suggest that addition of submicromolar concentrations of LEDGINs during virus production results in viruses that after integration are again refractory to LTR-driven gene expression (Supplementary Fig. 7), suggesting that during multiple round replication also low concentrations of LEDGINs induce quiescent proviral pools. Our data were corroborated with wt NL4.3 virus in IL-2/PHA activated primary CD4$^+$ T-cells (Fig. 7). These multiple round experiments allowed the use of submicromolar LEDGIN (CX014442) concentrations. It will be of interest to extend these observations in the future to other latency models. Preliminary data in a more sophisticated model for HIV latency based on infection of CCL19-activated resting CD4$^+$ cells (Spina et al., 2013) corroborates a LEDGIN-mediated shift of the HIV reservoir into a quiescent state refractory to reactivation (unpublished data). Evidence is growing that initiation of cART early after infection is effective in reducing the size of the viral reservoir (Ananworanich et al., 2012, 2015; Hocqueloux et al., 2013; Hoen et al., 2007; Malatinkova et al., 2015). Early treatment initiation with ART will likely become standard clinical practice in HIV care. This is supported by the outcome of the first large-scale international "Strategic Timing of AntiRetroviral Treatment" (START) study, showing a considerably lower risk of developing AIDS and other serious conditions when compared to later treatment initiation (INSIGHT START Study Group, 2015).

We here propose that LEDGINs, currently in (pre-)clinical development as antivirals, could eventually and in synergy with existing antiretrovirals contribute to an HIV remission by acting as potent antivirals with the additional capacity to affect the transcriptional state of the residual HIV reservoir. In an ideal format LEDGINs should be evaluated in combination with cART regimens initiated during acute infection before reservoirs are established. In light of recent findings on ongoing HIV replication, penetration of drugs in lymph nodes will be required. For HIV pre-exposure prophylaxis (PrEP) LEDGINs have the added benefit that any residual provirus may turn out to be refractory to reactivation. It is clear that this final outcome utterly depends on well-designed clinical trials and surpasses any claims made in this work. Still, we provide initial evidence in cell culture and primary cells for an important role of LEDGF/p75 in the establishment of the replicating reservoir. LEDGINs will allow us to investigate in clinical trials a novel strategy based on a retargeted, more quiescent proviral reservoir. LEDGIN treatment during acute HIV infection may result in proviruses that are refractory to reactivation after treatment interruption leading to an HIV remission.

Author Contributions

Z.D. conceived the study. L.V., A.B., S.S., G.V., C.W. and R.S. designed and conducted cell culture experiments. L.V., A.B, S.S., G.V., C.W., R.S., A.C., F.C., R.G. and Z.D analyzed the data. J.D and L.V. performed bioinformatic analyses. E.B., E.V, R.G. and R.S. cloned and designed the different reporter viruses. L.V., F.C., R.G. and Z.D. prepared the manuscript. Z.D. and R.G. were responsible for the coordination of the study. All authors read, corrected, and approved the final manuscript.

Disclosure

F.C. and Z.D. are inventors on LEDGIN patent applications but the specific compounds used in this paper do not fall under those patent applications.

References

Albanese, A., Arosio, D., Terreni, M., Cereseto, A., 2008. HIV-1 pre-integration complexes selectively target decondensed chromatin in the nuclear periphery. PLoS One 3, e2413.

Ananworanich, J., Dubé, K., Chomont, N., 2015. How does the timing of antiretroviral therapy initiation in acute infection affect HIV reservoirs? Curr. Opin. HIV AIDS 10, 18–28.

Ananworanich, J., Schuetz, A., Vandergeeten, C., Sereti, I., de Souza, M., Rerknimitr, R., Dewar, R., Marovich, M., van Griensven, F., Sekaly, R., et al., 2012. Impact of multi-targeted antiretroviral treatment on gut T cell depletion and HIV reservoir seeding during acute HIV infection. PLoS One 7, e33948.

Archin, N.M., Sung, J.M., Garrido, C., Soriano-Sarabia, N., Margolis, D.M., 2014. Eradicating HIV-1 infection: seeking to clear a persistent pathogen. Nat. Rev. Microbiol. 12, 750–764.

Balakrishnan, M., Yant, S.R., Tsai, L, O'Sullivan, C., Bam, R.A., Tsai, A., Niedziela-Majka, A., Stray, K.M., Sakowicz, R., Cihlar, T., 2013. Non-catalytic site HIV-1 integrase inhibitors disrupt core maturation and induce a reverse transcription block in target cells. PLoS One 8, e74163.

Borrenberghs, D., Thys, W., Rocha, S., Demeulemeester, J., Weydert, C., Dedecker, P., Hofkens, J., Debyser, Z., Hendrix, J., 2014. HIV virions as nanoscopic test tubes for probing oligomerization of the integrase enzyme. ACS Nano 8, 3531–3545.

Bruner, K.M., Hosmane, N.N., Siliciano, R.F., 2015. Towards an HIV-1 cure: measuring the latent reservoir. Trends Microbiol. 23, 192–203.

Butler, S.L., Hansen, M.S., Bushman, F.D., 2001. A quantitative assay for HIV DNA integration in vivo. Nat. Med. 7, 631–634.

Calvanese, V., Chavez, L., Laurent, T., Ding, S., Verdin, E., 2013. Dual-color HIV reporters trace a population of latently infected cells and enable their purification. Virology 446, 283–292.

Cavazzana-Calvo, M., Payen, E., Negre, O., Wang, G., Hehir, K., Fusil, F., Down, J., Denaro, M., Brady, T., Westerman, K., et al., 2010. Transfusion independence and HMGA2 activation after gene therapy of human β-thalassaemia. Nature 467, 318–322.

Chavez, L., Calvanese, V., Verdin, E., 2015. HIV latency is established directly and early in both resting and activated primary CD4 T cells. PLoS Pathog. 11, e1004955.

Cherepanov, P., Maertens, G., Proost, P., Devreese, B., Van Beeumen, J., Engelborghs, Y., De Clercq, E., Debyser, Z., 2003. HIV-1 integrase forms stable tetramers and associates with LEDGF/p75 protein in human cells. J. Biol. Chem. 278, 372–381.

Cherepanov, P., Sun, Z.-Y.J., Rahman, S., Maertens, G., Wagner, G., Engelman, A., 2005. Solution structure of the HIV-1 integrase-binding domain in LEDGF/p75. Nat. Struct. Mol. Biol. 12, 526–532.

Christ, F., Debyser, Z., 2013. The LEDGF/p75 integrase interaction, a novel target for anti-HIV therapy. Virology 435, 102–109.

Christ, F., Shaw, S., Demeulemeester, J., Desimmie, B.A., Marchand, A., Butler, S., Smets, W., Chaltin, P., Westby, M., Debyser, Z., et al., 2012. Small-molecule inhibitors of the LEDGF/p75 binding site of integrase block HIV replication and modulate integrase multimerization. Antimicrob. Agents Chemother. 56, 4365–4374.

Christ, F., Voet, A., Marchand, A., Nicolet, S., Desimmie, B.A., Marchand, D., Bardiot, D., Van der Veken, N.J., Van Remoortel, B., Strelkov, S.V., et al., 2010. Rational design of small-molecule inhibitors of the LEDGF/p75–integrase interaction and HIV replication. Nat. Chem. Biol. 6, 442–448.

Chun, T.W., Carruth, L., Finzi, D., Shen, X., DiGiuseppe, J.A., Taylor, H., Hermankova, M., Chadwick, K., Margolick, J., Quinn, T.C., et al., 1997a. Quantification of latent tissue reservoirs and total body viral load in HIV-1 infection. Nature 387, 183–188.

Chun, T.W., Stuyver, L., Mizell, S.B., Ehler, L.A., Mican, J.A., Baseler, M., Lloyd, A.L., Nowak, M.A., Fauci, A.S., 1997b. Presence of an inducible HIV-1 latent reservoir during highly active antiretroviral therapy. Proc. Natl. Acad. Sci. U. S. A. 94, 13193–13197.

Ciuffi, A., Llano, M., Poeschla, E., Hoffmann, C., Leipzig, J., Shinn, P., Ecker, J.R., Bushman, F., 2005. A role for LEDGF/p75 in targeting HIV DNA integration. Nat. Med. 11, 1287–1289.

Dahabieh, M.S., Battivelli, E., Verdin, E., 2015. Understanding HIV latency: the road to an HIV cure. Annu. Rev. Med. 66, 407–421.

Dahabieh, M.S., Ooms, M., Simon, V., Sadowski, I., 2013. A doubly fluorescent HIV-1 reporter shows that the majority of integrated HIV-1 is latent shortly after infection. J. Virol. 87, 4716–4727.

De Ravin, S.S., Su, L., Theobald, N., Choi, U., Macpherson, J.L., Poidinger, M., Symonds, G., Pond, S.M., Ferris, A.L., Hughes, S.H., et al., 2014. Enhancers are major targets for murine leukemia virus vector integration. J. Virol. 88, 4504–4513.

Debyser, Z., Christ, F., De Rijck, J., Gijsbers, R., 2015. Host factors for retroviral integration site selection. Trends Biochem. Sci. 40, 108–116.

Demeulemeester, J., Chaltin, P., Marchand, A., De Maeyer, M., Debyser, Z., Christ, F., 2014a. LEDGINs, non-catalytic site inhibitors of HIV-1 integrase: a patent review (2006–2014). Expert Opin. Ther. Pat. 24, 609–632.

Demeulemeester, J., De Rijck, J., Gijsbers, R., Debyser, Z., 2015. Retroviral integration: site matters: mechanisms and consequences of retroviral integration site selection. BioEssays (n/a–n/a).

Demeulemeester, J., Vets, S., Schrijvers, R., Madlala, P., De Maeyer, M., De Rijck, J., Ndung'u, T., Debyser, Z., Gijsbers, R., 2014b. HIV-1 integrase variants retarget viral integration and are associated with disease progression in a chronic infection cohort. Cell Host Microbe 16, 651–662.

Desimmie, B.A., Schrijvers, R., Demeulemeester, J., Borrenberghs, D., Weydert, C., Thys, W., Vets, S., Van Remoortel, B., Hofkens, J., De Rijck, J., et al., 2013. LEDGINs inhibit late stage HIV-1 replication by modulating integrase multimerization in the virions. Retrovirology 10, 57.

Di Primio, C., Quercioli, V., Allouch, A., Gijsbers, R., Christ, F., Debyser, Z., Arosio, D., Cereseto, A., 2013. Single-cell imaging of HIV-1 provirus (SCIP). Proc. Natl. Acad. Sci. U. S. A. 110, 5636–5641.

Eidahl, J.O., Crowe, B.L., North, J.A., McKee, C.J., Shkriabai, N., Feng, L., Plumb, M., Graham, R.L., Gorelick, R.J., Hess, S., et al., 2013. Structural basis for high-affinity binding of LEDGF PWWP to mononucleosomes. Nucleic Acids Res. 41, 3924–3936.

Fadel, H.J., Morrison, J.H., Saenz, D.T., Fuchs, J.R., Kvaratskhelia, M., Ekker, S.C., Poeschla, E.M., 2014. TALEN knockout of the PSIP1 gene in human cells: analyses of HIV-1 replication and allosteric integrase inhibitor mechanism. J. Virol. 88, 9704–9717.

Fader, L.D., Malenfant, E., Parisien, M., Carson, R., Bilodeau, F., Landry, S., Pesant, M., Brochu, C., Morin, S., Chabot, C., et al., 2014. Discovery of BI 224436, a noncatalytic site integrase inhibitor (NCINI) of HIV-1. ACS Med. Chem. Lett. 5, 422–427.

Fehse, B., Richters, A., Putimtseva-Scharf, K., Klump, H., Li, Z., Ostertag, W., Zander, A.R., Baum, C., 2000. CD34 splice variant: an attractive marker for selection of gene-modified cells. Mol. Ther. 1, 448–456.

Feng, L., Dharmarajan, V., Serrao, E., Hoyte, A., Larue, R.C., Slaughter, A., Sharma, A., Plumb, M.R., Kessl, J.J., Fuchs, J.R., et al., 2016. The competitive interplay between allosteric HIV-1 integrase inhibitor BI/D and LEDGF/p75 during the early stage of HIV-1 replication adversely affects inhibitor potency. ACS Chem. Biol.

Fenwick, C., Amad, M., Bailey, M.D., Bethell, R., Bös, M., Bonneau, P., Cordingley, M., Coulombe, R., Duan, J., Edwards, P., et al., 2014. Preclinical profile of BI 224436, a novel HIV-1 non-catalytic-site integrase inhibitor. Antimicrob. Agents Chemother. 58, 3233–3244.

Finzi, D., Hermankova, M., Pierson, T., Carruth, L.M., Buck, C., Chaisson, R.E., Quinn, T.C., Chadwick, K., Margolick, J., Brookmeyer, R., et al., 1997. Identification of a reservoir for HIV-1 in patients on highly active antiretroviral therapy. Science 278, 1295–1300.

Francis, A.C., Di Primio, C., Quercioli, V., Valentini, P., Boll, A., Girelli, G., Demichelis, F., Arosio, D., Cereseto, A., 2014. Second generation imaging of nuclear/cytoplasmic HIV-1 complexes. AIDS Res. Hum. Retrovir. 30, 717–726.

Gérard, A., Ségéral, E., Naughtin, M., Abdouni, A., Charmeteau, B., Cheynier, R., Rain, J.-C., Emiliani, S., 2015. The integrase cofactor LEDGF/p75 associates with Iws1 and Spt6 for postintegration silencing of HIV-1 gene expression in latently infected cells. Cell Host Microbe 17, 107–117.

Gijsbers, R., Ronen, K., Vets, S., Malani, N., De Rijck, J., McNeely, M., Bushman, F.D., Debyser, Z., 2009. LEDGF hybrids efficiently retarget lentiviral integration into heterochromatin. Mol. Ther. 18, 552–560.

Gupta, K., Brady, T., Dyer, B.M., Malani, N., Hwang, Y., Male, F., Nolte, R.T., Wang, L., Velthuisen, E., Jeffrey, J., et al., 2014. Allosteric inhibition of human immunodeficiency virus integrase: late block during viral replication and abnormal multimerization involving specific protein domains. J. Biol. Chem. 289, 20477–20488.

Han, Y., Lassen, K., Monie, D., Sedaghat, A.R., Shimoji, S., Liu, X., Pierson, T.C., Margolick, J.B., Siliciano, R.F., Siliciano, J.D., 2004. Resting CD4 + T cells from human immunodeficiency virus type 1 (HIV-1)-infected individuals carry integrated HIV-1 genomes within actively transcribed host genes. J. Virol. 78, 6122–6133.

Hocqueloux, L., Avettand-Fènoël, V., Jacquot, S., Prazuck, T., Legac, E., Melard, A., Niang, M., Mille, C., Le Moal, G., Viard, J.-P., et al., 2013. Long-term antiretroviral therapy initiated during primary HIV-1 infection is key to achieving both low HIV reservoirs and normal T cell counts. J. Antimicrob. Chemother. 68, 1169–1178.

Hoen, B., Cooper, D.A., Lampe, F.C., Perrin, L., Clumeck, N., Phillips, A.N., Goh, L.-E., Lindback, S., Sereni, D., Gazzard, B., et al., 2007. Predictors of virological outcome and safety in primary HIV type 1-infected patients initiating quadruple antiretroviral therapy: QUEST GW PROB3005. Clin. Infect. Dis. 45, 381–390.

Holman, A.G., Coffin, J.M., 2005. Symmetrical base preferences surrounding HIV-1, avian sarcoma/leukosis virus, and murine leukemia virus integration sites. Proc. Natl. Acad. Sci. U. S. A. 102, 6103–6107.

Jordan, A., Defechereux, P., Verdin, E., 2001. The site of HIV-1 integration in the human genome determines basal transcriptional activity and response to Tat transactivation. EMBO J. 20, 1726–1738.

Jurado, K.A., Wang, H., Slaughter, A., Feng, L., Kessl, J.J., Koh, Y., Wang, W., Ballandras-Colas, A., Patel, P.A., Fuchs, J.R., et al., 2013. Allosteric integrase inhibitor potency is determined through the inhibition of HIV-1 particle maturation. Proc. Natl. Acad. Sci. U. S. A. 110, 8690–8695.

Kessl, J.J., Jena, N., Koh, Y., Taskent-Sezgin, H., Slaughter, A., Feng, L., de Silva, S., Wu, L., Le Grice, S.F.J., Engelman, A., et al., 2012. Multimode, cooperative mechanism of action of allosteric HIV-1 integrase inhibitors. J. Biol. Chem. 287, 16801–16811.

Le Rouzic, E., Bonnard, D., Chasset, S., Bruneau, J.-M., Chevreuil, F., Le Strat, F., Nguyen, J., Beauvoir, R., Amadori, C., Brias, J., et al., 2013. Dual inhibition of HIV-1 replication by integrase-LEDGF allosteric inhibitors is predominant at the post-integration stage. Retrovirology 10, 144.

Lelek, M., Casartelli, N., Pellin, D., Rizzi, E., Souque, P., Severgnini, M., Di Serio, C., Fricke, T., Diaz-Griffero, F., Zimmer, C., et al., 2015. Chromatin organization at the nuclear pore favours HIV replication. Nat. Commun. 6, 6483.

Lewin, S.R., Murray, J.M., Solomon, A., Wightman, F., Cameron, P.U., Purcell, D.J., Zaunders, J.J., Grey, P., Bloch, M., Smith, D., et al., 2008. Virologic determinants of success after structured treatment interruptions of antiretrovirals in acute HIV-1 infection. J. Acquir. Immune Defic. Syndr. 47, 140–147.

Liu, H., Dow, E.C., Arora, R., Kimata, J.T., Bull, L.M., Arduino, R.C., Rice, A.P., 2006. Integration of human immunodeficiency virus type 1 in untreated infection occurs preferentially within genes. J. Virol. 80, 7765–7768.

Lorenzo-Redondo, R., Fryer, H.R., Bedford, T., Kim, E.-Y., Archer, J., Kosakovsky Pond, S.L., Chung, Y.-S., Penugonda, S., Chipman, J.G., Fletcher, C.V., et al., 2016. Persistent HIV-1 replication maintains the tissue reservoir during therapy. Nature 530, 51–56.

Malatinkova, E., De Spiegelaere, W., Bonczkowski, P., Kiselinova, M., Vervisch, K., Trypsteen, W., Johnson, M., Verhofstede, C., de Looze, D., Murray, C., et al., 2015. Impact of a decade of successful antiretroviral therapy initiated at HIV-1 seroconversion on blood and rectal reservoirs. Elife 4.

Maldarelli, F., Wu, X., Su, L., Simonetti, F.R., Shao, W., Hill, S., Spindler, J., Ferris, A.L., Mellors, J.W., Kearney, M.F., et al., 2014. HIV latency. Specific HIV integration sites are linked to clonal expansion and persistence of infected cells. Science 345, 179–183.

Marini, B., Kertesz-Farkas, A., Ali, H., Lucic, B., Lisek, K., Manganaro, L., Pongor, S., Luzzati, R., Recchia, A., Mavilio, F., et al., 2015. Nuclear architecture dictates HIV-1 integration site selection. Nature 521, 227–231.

Marshall, H.M., Ronen, K., Berry, C., Llano, M., Sutherland, H., Saenz, D., Bickmore, W., Poeschla, E., Bushman, F.D., 2007. Role of PSIP1/LEDGF/p75 in lentiviral infectivity and integration targeting. PLoS One 2, e1340.

Mitchell, R.S., Beitzel, B.F., Schroder, A.R.W., Shinn, P., Chen, H., Berry, C.C., Ecker, J.R., Bushman, F.D., 2004. Retroviral DNA integration: ASLV, HIV, and MLV show distinct target site preferences. PLoS Biol. 2, e234.

Ocwieja, K.E., Brady, T.L., Ronen, K., Huegel, A., Roth, S.L., Schaller, T., James, L.C., Towers, G.J., Young, J.A.T., Chanda, S.K., et al., 2011. HIV integration targeting: a pathway involving transportin-3 and the nuclear pore protein RanBP2. PLoS Pathog. 7, e1001313–e1001314.

Osório, L., Gijsbers, R., Oliveras-Salvá, M., Michiels, A., Debyser, Z., Van den Haute, C., Baekelandt, V., 2014. Viral vectors expressing a single microRNA-based short-hairpin RNA result in potent gene silencing in vitro and in vivo. J. Biotechnol. 169, 71–81.

Papapetrou, E.P., Lee, G., Malani, N., Setty, M., Riviere, I., Tirunagari, L.M.S., Kadota, K., Roth, S.L., Giardina, P., Viale, A., et al., 2011. Genomic safe harbors permit high β-globin transgene expression in thalassemia induced pluripotent stem cells. Nat. Biotechnol. 29, 73–78.

Pizzato, M., Erlwein, O., Bonsall, D., Kaye, S., Muir, D., McClure, M.O., 2009. A one-step SYBR Green I-based product-enhanced reverse transcriptase assay for the quantitation of retroviruses in cell culture supernatants. J. Virol. Methods 156, 1–7.

Pradeepa, M.M., Sutherland, H.G., Ule, J., Grimes, G.R., Bickmore, W.A., 2012. Psip1/Ledgf p52 binds methylated histone H3K36 and splicing factors and contributes to the regulation of alternative splicing. PLoS Genet. 8, e1002717.

Razooky, B.S., Pai, A., Aull, K., Rouzine, I.M., Weinberger, L.S., 2015. A hardwired HIV latency program. Cell 160, 990–1001.

Richman, D.D., Margolis, D.M., Delaney, M., Greene, W.C., Hazuda, D., Pomerantz, R.J., 2009. The challenge of finding a cure for HIV infection. Science 323, 1304–1307.

Rouzine, I.M., Weinberger, A.D., Weinberger, L.S., 2015. An evolutionary role for HIV latency in enhancing viral transmission. Cell 160, 1002–1012.

Saleh, S., Wightman, F., Ramanayake, S., Alexander, M., Kumar, N., Khoury, G., Pereira, C., Purcell, D., Cameron, P.U., Lewin, S.R., 2011. Expression and reactivation of HIV in a chemokine induced model of HIV latency in primary resting CD4 + T cells. Retrovirology 8, 80.

Sallusto, F., Lenig, D., Förster, R., Lipp, M., Lanzavecchia, A., 1999. Two subsets of memory T lymphocytes with distinct homing potentials and effector functions. Nature 401, 708–712.

Schrijvers, R., De Rijck, J., Demeulemeester, J., Adachi, N., Vets, S., Ronen, K., Christ, F., Bushman, F.D., Debyser, Z., Gijsbers, R., 2012a. LEDGF/p75-independent HIV-1 replication demonstrates a role for HRP-2 and remains sensitive to inhibition by LEDGINs. PLoS Pathog. 8, e1002558.

Schrijvers, R., Vets, S., De Rijck, J., Malani, N., Bushman, F.D., Debyser, Z., Gijsbers, R., 2012b. HRP-2 determines HIV-1 integration site selection in LEDGF/p75 depleted cells. Retrovirology 9, 84.

Schroder, A.R.W., Shinn, P., Chen, H., Berry, C., Ecker, J.R., Bushman, F., 2002. HIV-1 integration in the human genome favors active genes and local hotspots. Cell 110, 521–529.

Serrao, E., Ballandras-Colas, A., Cherepanov, P., Maertens, G.N., Engelman, A.N., 2015. Key determinants of target DNA recognition by retroviral intasomes. Retrovirology 12, 39.

Shan, L., Yang, H.-C., Rabi, S.A., Bravo, H.C., Shroff, N.S., Irizarry, R.A., Zhang, H., Margolick, J.B., Siliciano, J.D., Siliciano, R.F., 2011. Influence of host gene transcription level and orientation on HIV-1 latency in a primary-cell model. J. Virol. 85, 5384–5393.

Sharma, A., Slaughter, A., Jena, N., Feng, L., Kessl, J.J., Fadel, H.J., Malani, N., Male, F., Wu, L., Poeschla, E., et al., 2014. A new class of multimerization selective inhibitors of HIV-1 integrase. PLoS Pathog. 10, e1004171.

Shun, M.-C., Raghavendra, N.K., Vandegraaff, N., Daigle, J.E., Hughes, S., Kellam, P., Cherepanov, P., Engelman, A., 2007. LEDGF/p75 functions downstream from preintegration complex formation to effect gene-specific HIV-1 integration. Genes Dev. 21, 1767–1778.

Siliciano, J.M., Siliciano, R.F., 2015. The remarkable stability of the latent reservoir for HIV-1 in resting memory CD4 + T cells. J. Infect. Dis.

Spina, C.A., Anderson, J., Archin, N.M., Bosque, A., Chan, J., Famiglietti, M., Greene, W.C., Kashuba, A., Lewin, S.R., Margolis, D.M., et al., 2013. An in-depth comparison of latent

HIV-1 reactivation in multiple cell model systems and resting CD4+ T cells from aviremic patients. PLoS Pathog. 9, e1003834.

The INSIGHT START Study Group, 2015. Initiation of Antiretroviral Therapy in Early Asymptomatic HIV Infection. N. Engl. J. Med. 373, 795–807.

Tsiang, M., Jones, G.S., Niedziela-Majka, A., Kan, E., Lansdon, E.B., Huang, W., Hung, M., Samuel, D., Novikov, N., Xu, Y., et al., 2012. New class of HIV-1 integrase (IN) inhibitors with a dual mode of action. J. Biol. Chem. 287, 21189–21203.

Vandekerckhove, L., Christ, F., Van Maele, B., De Rijck, J., Gijsbers, R., Van den Haute, C., Witvrouw, M., Debyser, Z., 2006. Transient and stable knockdown of the integrase cofactor LEDGF/p75 reveals its role in the replication cycle of human immunodeficiency virus. J. Virol. 80, 1886–1896.

Wagner, T.A., McLaughlin, S., Garg, K., Cheung, C.Y.K., Larsen, B.B., Styrchak, S., Huang, H.C., Edlefsen, P.T., Mullins, J.I., Frenkel, L.M., 2014. HIV latency. Proliferation of cells with HIV integrated into cancer genes contributes to persistent infection. Science 345, 570–573.

Wang, H., Jurado, K.A., Wu, X., Shun, M.-C., Li, X., Ferris, A.L., Smith, S.J., Patel, P.A., Fuchs, J.R., Cherepanov, P., et al., 2012. HRP2 determines the efficiency and specificity of HIV-1 integration in LEDGF/p75 knockout cells but does not contribute to the antiviral activity of a potent LEDGF/p75-binding site integrase inhibitor. Nucleic Acids Res. 40, 11518–11530.

Zhang, Z., Schuler, T., Zupancic, M., Wietgrefe, S., Staskus, K.A., Reimann, K.A., Reinhart, T.A., Rogan, M., Cavert, W., Miller, C.J., et al., 1999. Sexual transmission and propagation of SIV and HIV in resting and activated CD4+ T cells. Science 286, 1353–1357.